

ABSTRACT

Title of Document: TRACING RETROGRADE METAMORPHIC FLUIDS IN A SUBDUCTION ZONE USING LI: FRANCISCAN COMPLEX, CALIFORNIA

John-Luke Henriquez, M.S., 2012

Directed By: Dr. Sarah C. Penniston-Dorland, Geology
Dr. William F. McDonough, Geology

Centimeter-scale layers of eclogite and blueschist from Tiburon Peninsula, Franciscan Complex, CA were contrasted with a similarly layered sample from Dos Rios, CA. Eclogites from both localities have similar mineral assemblages (e.g., omphacite, glaucophane, phengite, garnet, epidote, and titanite). However, the Tiburon blueschist shows petrographic evidence for fluid-rock interaction, while the Dos Rios sample does not. Mineral phases common to both samples were contrasted via textural evidence, major and minor element concentrations, and lithium concentrations. Lithium concentrations of omphacite and chlorite decrease from the eclogite to the blueschist domains in the Tiburon sample. These lithium concentration differences are interpreted to be the result of fluid-rock interactions. These differences are not seen in the Dos Rios sample. I propose that a difference in the Dos Rios sample bulk composition produced the alternating eclogite and blueschist lithologies as a result of a process such as seafloor alteration prior to prograde metamorphism.

TRACING RETROGRADE METAMORPHIC FLUIDS IN A SUBDUCTION
ZONE USING LI: FRANCISCAN COMPLEX, CALIFORNIA

By

John-Luke Henriquez

Thesis submitted to the Faculty of the Graduate School of the
University of Maryland, College Park, in partial fulfillment
of the requirements for the degree of
Master of Science
2012

Advisory Committee:
Professor Sarah C. Penniston-Dorland, Co-Chair
Professor William F. McDonough, Co-Chair
Senior Research Scientist Philip M. Piccoli

© Copyright by
John-Luke Henriquez
2012

Table of Contents

Table of Contents	ii
List of Tables	iv
List of Figures	v
1 Introduction.....	1
2 Geologic background	4
2.1 Retrograde metamorphism in the Franciscan Complex	6
2.2 Samples	7
3 Methods.....	10
3.1 Petrography	10
3.2 Electron Probe Microanalyzer (EPMA).....	10
3.3 Laser Ablation Inductively Coupled Mass Spectrometry (LA-ICP-MS)	11
3.4 Error analyses.....	12
3.4.1 Point counting	12
3.4.2 EPMA.....	13
3.4.3 LA-ICP-MS.....	13
3.4.4 Error propagation	14
4 Results.....	15
4.1 Textural observations	15
4.1.1 Tiburon.....	15
4.1.2 Dos Rios	16
4.2 EPMA Results.....	18
4.2.1 Amphibole.....	18
4.2.2 Omphacite	21
4.2.3 Phengite.....	24
4.2.4 Chlorite.....	28
4.2.5 Low-Li phases.....	30
4.3 LA-ICP-MS Results	30
4.3.1 Amphibole.....	31
4.3.2 Omphacite	32
4.3.3 Phengite.....	33
4.3.4 Chlorite.....	35
4.3.5 Low-Li phases.....	36
4.4 Bulk rock reconstruction.....	37
5 Discussion.....	39
5.1 Textural observations	39

5.2	Major and minor element mineral compositions	40
5.3	Li concentration analysis results	41
5.4	Comparison to other studies.....	41
5.5	Possible mechanisms for coexisting blueschist and eclogite in Dos Rios sample 42	
6	Conclusions	47
7	Appendices.....	50
8.1	Appendix A: Tiburon data tables	50
8.2	Appendix B: Dos Rios data.....	50
8.3	Appendix C: Accuracy and precision data.....	50
8	References	51

List of Tables

Table 1. Results of point counting of Tiburon sample.....	8
Table 2. Results of point counting of Dos Rios sample.....	8
Table 3. Standards used in EPMA analyses.....	11
Table 4. EPMA results for major Li-bearing phases in Tiburon sample.....	19
Table 5. EPMA results for major Li-bearing phases in Tiburon sample.....	20
Table 6. Range of Li concentrations measured in this study for individual minerals in this study and in Marschall et al. (2006).....	42

List of Figures

Figure 1. Sample locality map	1
Figure 2. Comparison of Li concentration of two samples.	3
Figure 3. Photomicrographs of samples.	4
Figure 4. BSE images of Tiburon sample	6
Figure 5. Bulk rock Li concentration of Tiburon samples.	9
Figure 6. Comparison of garnets from contact distance in Tiburon sample.	17
Figure 7. Amphibole composition chart	22
Figure 8. Omphacite composition chart.....	23
Figure 9. Mg vs Si in phengites.	25
Figure 10. Na vs Si in phengites.	26
Figure 11. Chlorite composition chart.	29
Figure 12. Tiburon amphibole Li concentrations.	31
Figure 13. Dos Rios amphibole Li concentrations.....	32
Figure 14. Tiburon omphacite Li concentrations.	33
Figure 15. Dos Rios omphacite Li concentrations.	34
Figure 16. Tiburon phengite Li concentrations.....	34
Figure 17. Dos Rios phengite Li concentrations.	35
Figure 18. Tiburon chlorite Li concentrations.	36
Figure 19. Tiburon bulk rock reconstruction	38
Figure 20. Dos Rios bulk rock reconstruction.	38

1 Introduction

Subduction zone fluids play a pronounced role in geologic processes such as plate tectonics, and the production of the continental crust. Fluids also play an important role in element cycling in the crust and subcontinental lithospheric mantle. As the subducting slab is exposed to pressure and temperature changes, elements are transferred from the slab to the overlying mantle by fluids and/or melts. This process ultimately leads to the production of island arc volcanoes and the formation of the continental crust (Manning, 2004), and is related to

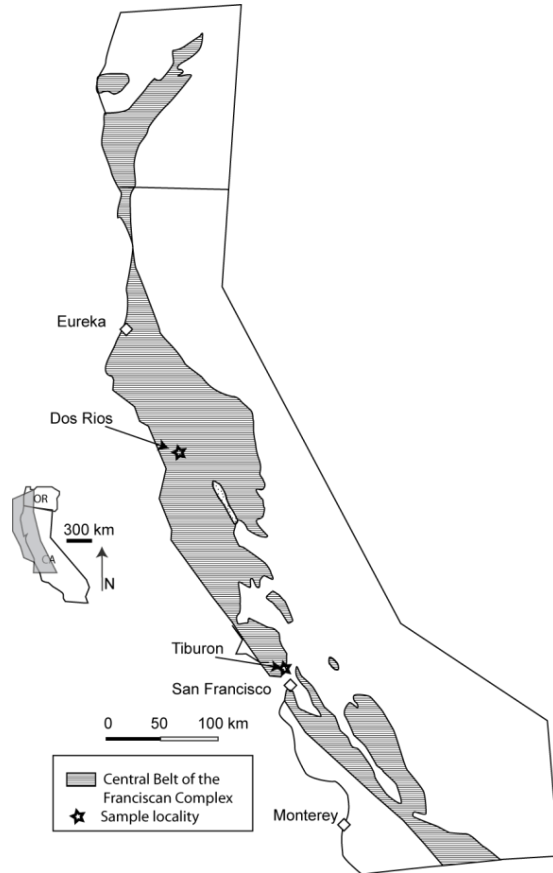


Figure 1. Simplified sample locality map after Sorensen et al. (1997).

processes that include tectonic plate motion and seismicity. Tracing the record left behind in metamorphic rocks by subduction zone fluids can help answer questions about: (i) fluid flow pathways and mechanisms of fluid flow (e.g., intergranular flow or fracture flow) in subduction zones; (ii) sources of fluids in the subduction zone (e.g., fluids from subducted sea water, fluids derived from mineral dehydration in the oceanic crust, or fluids rising from the oceanic lithospheric mantle); (iii) mobility of

elements in subduction zone fluids; and (iv) time scales of subduction zone fluid flow. Mélange zones are areas where fluids can traverse and exchange elements among the downgoing slab, the overlying mantle wedge, and the material that breaks off and mechanically mixes between these two domains (Bebout, 2007; Cloos, 1986).

Lithium is a moderately incompatible lithophile trace element with an average composition in oceanic crust estimated to be 10 $\mu\text{g/g}$ and an average composition in the bulk continental crust estimated to be 18 $\mu\text{g/g}$ (Teng et al., 2008). Lithium partitions strongly into an aqueous phase at high pressure-temperature conditions (Brenan et al., 1998). This behavior has allowed previous studies to use lithium to monitor fluid-rock interactions (e.g., Teng et al., 2006). Previous studies have used Li as a tracer of subduction zone processes and have identified at least three different processes that produce Li differentiation in subduction zone rocks: diffusion (Marschall et al., 2007), dehydration (Zack et al., 2003), and fluid infiltration (Penniston-Dorland et al., 2010).

In this study, two samples from the Franciscan Complex were examined – one from the Tiburon Peninsula, California (T90-3A) and the other from Dos Rios, California (samples courtesy of Sorena Sorensen, Smithsonian Institution, Washington, DC; Figure 1.). Both samples have cm-scale domains of eclogite and blueschist. In both samples, the change from eclogite to blueschist correlates with a change in bulk rock Li concentration (Figure 2). This change in Li concentration in the Tiburon sample is interpreted as the product of fluid infiltration (Penniston-Dorland et al., 2010) since the blueschist layer in the Tiburon sample has petrologic evidence of fluid-induced, retrograde metamorphism, including chlorite after garnet

pseudomorphs. The blueschist layer in the Dos Rios sample, on the other hand, does not have similar evidence for fluid-induced metamorphism. The questions to be addressed in this study are: i) Does the Li concentration of individual minerals vary in concert with the bulk rock Li concentration in the samples? ii) Did the blueschist in the Dos Rios sample undergo fluid-induced, retrograde metamorphism similar to the blueschist in the Tiburon sample? If not, iii) by what mechanism was the blueschist in the Dos Rios sample

generated and iv) why is the Li concentration in blueschist domains different than in the eclogite domains in the Dos Rios samples. To answer these questions, the petrography and the major and minor element chemistry of phases in the

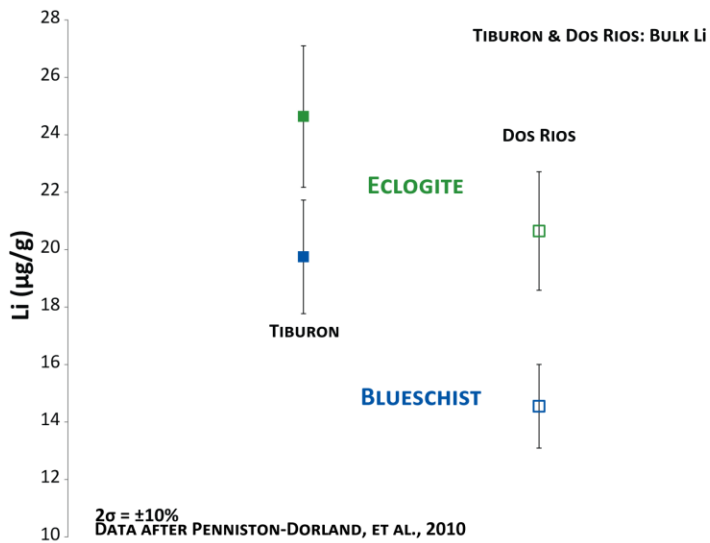


Figure 2. In the Tiburon and Dos Rios samples, the blueschist domain has a lower Li concentration than their associated eclogite domains. Uncertainty for the Li concentration measurements is $\pm 10\%$ (Penniston-Dorland et al., 2010).

samples were analyzed in both eclogite and blueschist domains (blue amphibole, chlorite, omphacite, phengite, garnet, epidote, and titanite). In each phase, the Li concentration was analyzed in order to get an accurate determination of Li budget in the rocks. A comparison of Li concentration in phases across the eclogite-blueschist interface in each sample will demonstrate whether the bulk rock variations are more likely due to differences in mineral modes (Li concentration in a given mineral phase

will not vary significantly between layers) or due to exchange of Li with an intergranular fluid (Li concentration in a given mineral phase in fluid-altered rock layers will differ in altered layers compared to associated unaltered layers

2 Geologic background

Mélange zones are hypothesized as areas of mechanical mixing at the interface between the mantle wedge and downgoing crustal slab (Bebout, 2007; Cloos, 1986). Mélange zones consist of meter-scale high-grade blocks of blueschist, eclogite, garnet amphibolite, and/or graywacke entrained in a fine-grained metasedimentary or ultramafic matrix. They are found in many subduction zones around the world (e.g., the Franciscan Complex, California;

Samana Peninsula, Dominican Republic; Syros, Greece; Kyushu, Japan). The Franciscan Complex formed during the convergence of the North American and Pacific plates during a period of subduction that began between 150 and 153 Ma,

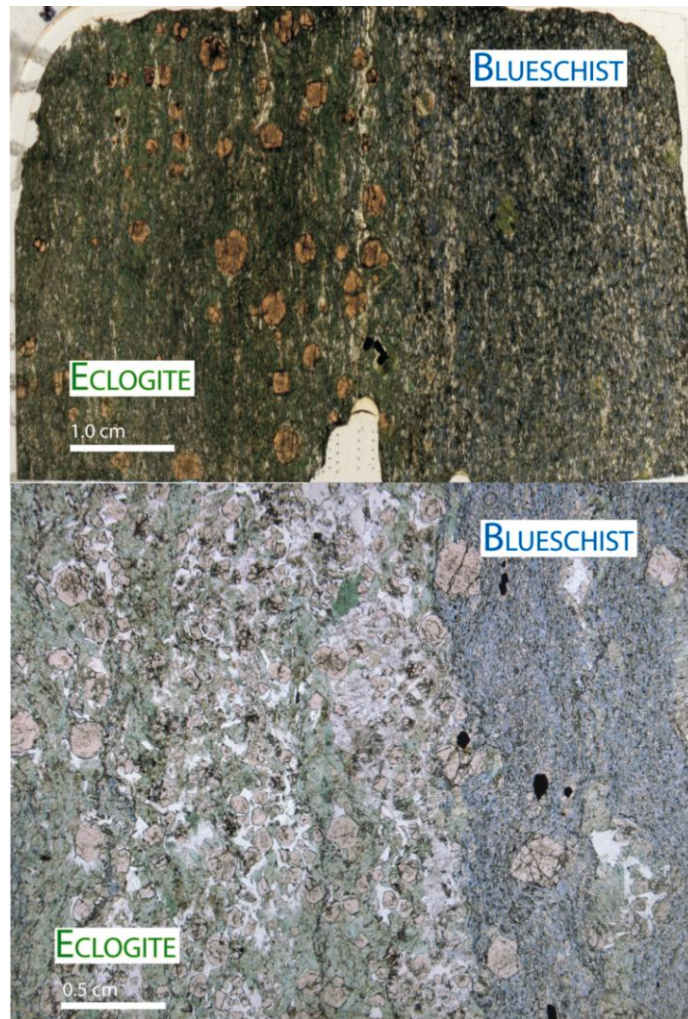


Figure 3. Transmitted light photomicrograph of the Tiburon sample (top, 3a) and plane polarized light photomicrograph of the Dos Rios sample (bottom, 3b).

during the Late Jurassic (Coleman and Lanphere, 1971; Nelson, 1991). The Franciscan Complex is split into Coastal, Central, and Eastern belts and the mélange zones found within the Western and Central belts contain high-grade blocks of blueschist and eclogite [T = 200 – 600 °C; P = 0.6 to 1.0 GPa (Cloos, 1986; Giaramita and Sorensen, 1994; Wakabayashi, 1990)]. Most of the blocks are reported to be found in a matrix of fine-grained, argillaceous metasedimentary rock (Cloos, 1983; Cloos, 1986; Moore and Blake, 1989). However, in the Tiburon and Dos Rios localities, the contact relations of these blocks with their immediate surroundings are unclear. The fine-grained matrix often weathers away, giving the landscape characteristic hummocks.

Most of the blocks have a Mg-rich, actinolitic rind, thought to have formed as a result of metasomatism from fluids derived from serpentized ultramafic rocks (Cloos, 1986; Nelson, 1995; Sorensen et al., 1997). Low ϵ_{Nd} and large ion lithophile element (LILE) enrichment in the rinds provide evidence that fluids derived from subducting sedimentary rocks were added (Nelson, 1995; Sorensen et al., 1997). $^{40}Ar/^{39}Ar$ ages from phengite grains in Franciscan Complex blocks indicate fluid-rock interactions continued for up to 60 million years (Catlos and Sorensen, 2003). The bulk rock major element composition and the concentrations of rare-earth elements (REE) and high-field strength elements (HFSE) show that most Franciscan blocks are similar in composition to mid-ocean ridge basalts, a likely protolith (Sorensen et al., 1997). In addition, the unaltered cores of these blocks have ϵ_{Nd} of 9.3 ± 1.4 , consistent with a normal depleted-mantle source (Nelson, 1995).

2.1 Retrograde metamorphism in the Franciscan Complex

Evidence for retrograde metamorphism in rocks is rarer than for prograde metamorphism. This is commonly due to: (i) lower temperatures after peak metamorphism, which leads to much slower reaction rates; (ii) lack of active tectonism after peak metamorphism; or (iii) lack of available fluids to mediate chemical reactions after peak metamorphism. There is, however, evidence of fluid-mediated retrograde metamorphism in the high-grade Franciscan Complex blocks, including: (i) chlorite after garnet pseudomorphs; (ii) replacement of epidote by pumpellyite; omphacite by glaucophane, chlorite, phengite, and lawsonite; (iii) the random orientation and cross-cutting of the foliation by the replacement minerals (Cloos, 1986; Nelson, 1995; Penniston-Dorland et al., 2010).

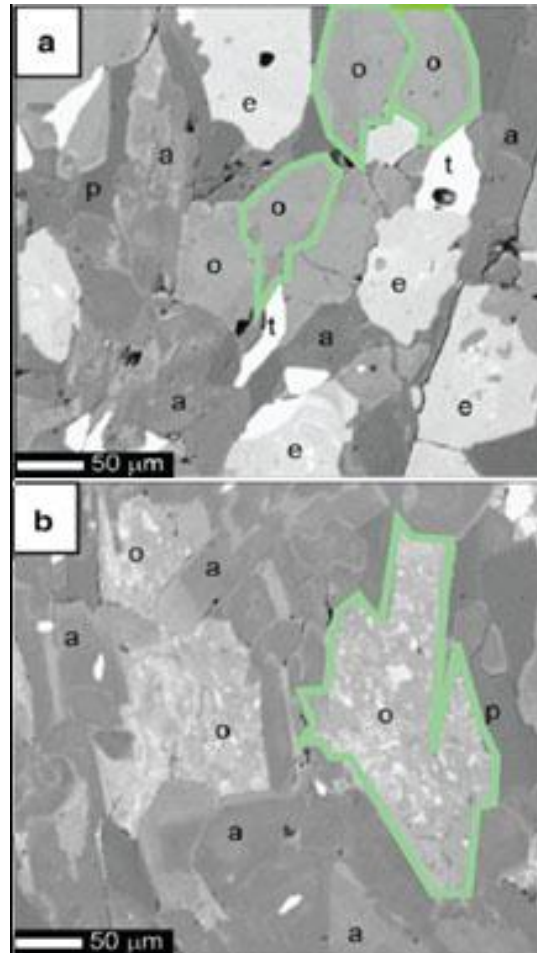


Figure 4. Backscattered electron (BSE) images of Tiburon omphacites after Penniston-Dorland, et al. (2010). ‘o’ indicates omphacites, ‘a’ indicates amphiboles, ‘p’ indicates phengite, and ‘e’ indicates epidotes. 4a shows the sodic, homogeneous texture of the omphacites in the eclogite domain. 4b shows the altered omphacites in the Dos Rios sample. The sodic omphacite has altered to diopside and pumpellyite, indicated by the light patches within the mineral.

2.2 Samples

The Tiburon sample has roughly equal eclogite and blueschist portions coexisting in the sample, separated by a sharp contact between the two (Figure 3a). The Dos Rios sample has multiple, cm-scale eclogite and blueschist regions (Figure 3b). The most common phases in both samples include omphacite, phengite, sodic amphibole, epidote, garnet, and titanite (See Tables 1 and 2). The blueschist domain of Tiburon shows evidence for fluid-induced, retrograde metamorphism. This evidence includes chlorite after garnet pseudomorphs and altered, “patchy” omphacites in the blueschist and the presence of pumpellyite in the blueschist layer (Figure 4a and 4b). In contrast, the Dos Rios sample has no distinct petrological evidence for fluid-induced, retrograde metamorphism in the blueschist: for example, there are no chlorite after garnet pseudomorphs and the omphacites are unaltered in the blueschist domains.

Penniston-Dorland et al. (2010) performed bulk Li concentration analyses on whole-rock slices cut along a traverse across the sample in the Tiburon sample (Figure 5). The authors found that the bulk Li concentration in the blueschist portion of the rock was consistently lower than that of the eclogite portion of the rock (17 – 20 $\mu\text{g/g}$ and 21 – 28 $\mu\text{g/g}$, respectively), indicating that the fluid that interacted with the blueschist depleted the rock in Li concentration.

The Dos Rios sample shows a similar difference in bulk Li concentration between blueschist and eclogite (13 – 16 $\mu\text{g/g}$ and 19 – 21 $\mu\text{g/g}$, respectively; Penniston-Dorland, unpublished data). The methods outlined here will be used to

Tiburon

Eclogite			
phase	count	% total	σ
Amphibole	256	13%	0.74%
Apatite	17	0.84%	0.20%
Chlorite	66	3.3%	0.39%
Epidote	292	14%	0.78%
Garnet	165	8.1%	0.61%
Omphacite	793	39%	1.1%
Phengite	356	18%	0.84%
Titanite	82	4.0%	0.44%
Total	2029	100%	
Blueschist			
phase	count	% total	σ
Amphibole	958	47%	1.1%
Apatite	17	0.83%	0.20%
Chlorite	198	9.7%	0.65%
Epidote	26	1.3%	0.25%
Garnet	2	0.1%	0.07%
Omphacite	183	8.9%	0.63%
Phengite	412	20%	0.89%
Pumpellyite	132	6.4%	0.54%
Titanite	108	5.3%	0.49%
Total	2049	100%	

Dos Rios

Eclogite			
Phase	Count	Vol. %	σ
Amphibole	296	15%	0.78%
Apatite	10	0.49%	0.16%
Chlorite	1	0.05%	0.05%
Epidote	435	21%	0.91%
Garnet	307	15%	0.79%
Omphacite	666	33%	1.0%
Phengite	241	12%	0.72%
Titanite	76	3.7%	0.42%
Total	2032	100%	
Blueschist			
Phase	Count	%	σ
Amphibole	1228	56%	1.10%
Apatite	10	0.46%	0.15%
Chlorite	1	0.05%	0.05%
Epidote	579	26%	0.98%
Garnet	111	5.1%	0.49%
Omphacite	96	4.4%	0.45%
Phengite	37	1.7%	0.29%
Titanite	125	5.7%	0.51%
Total	2187	100%	

Table 1 and Table 2. Results of point counting for eclogite (green) and blueschist (blue) of Tiburon (left) and Dos Rios (right) samples. 1σ is the absolute uncertainty, in modal percent, calculated after Van Der Plas and Tobi (1965). Refer to section on Error Analyses for an in-depth discussion about calculating uncertainty associated with point counting. Mineral modes were measured by Hanson and Penniston-Dorland (unpublished data) counting ≥ 2000 points in thin section with back-scattered electron (BSE) imaging using a JEOL JXA-8900 Superprobe electron probe microanalyzer.

Tiburon: Bulk Li vs distance from contact

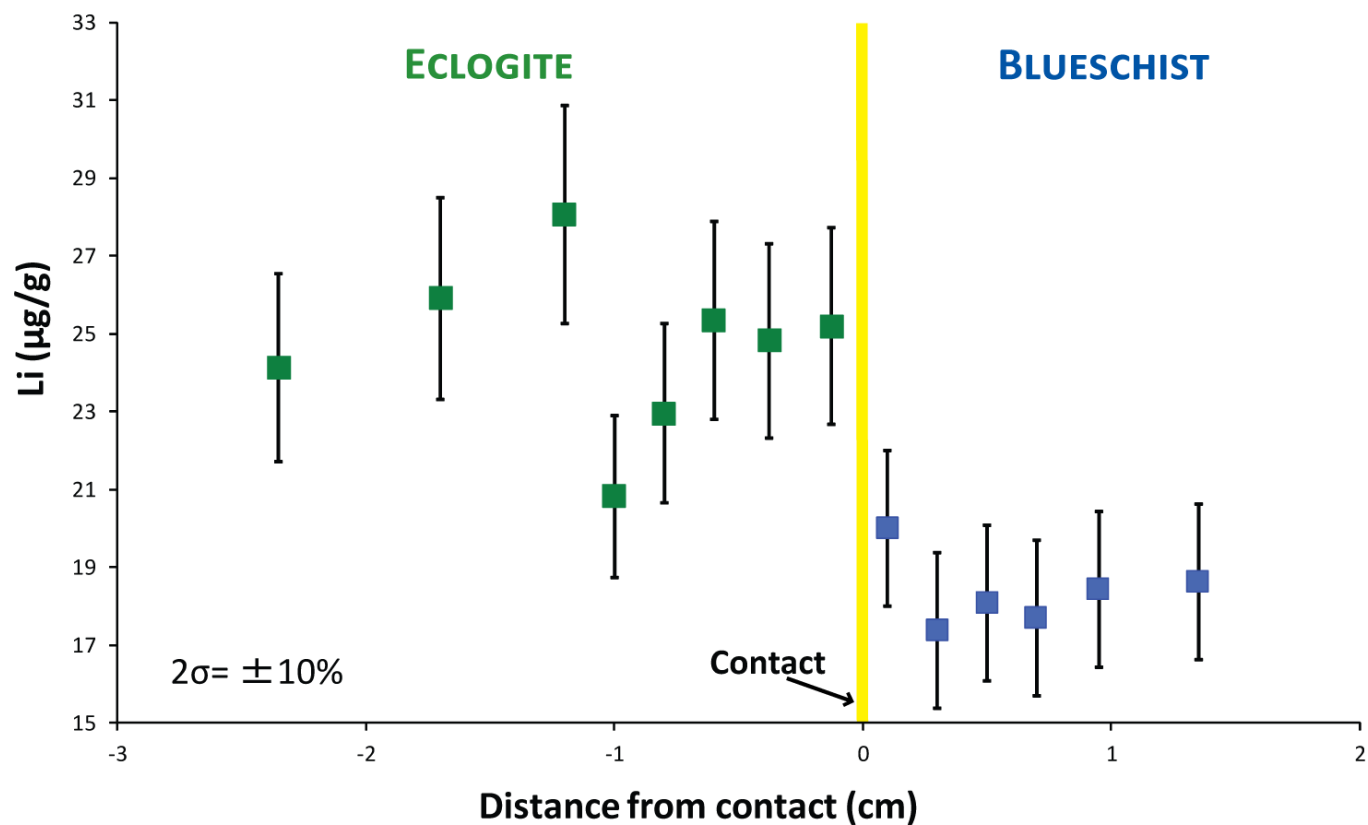


Figure 5. Bulk rock Li concentration in Tiburon sample. Bulk Li concentration generally decreases going from eclogite to blueschist domains. Data after Penniston-Dorland et al. (2010).

determine if the Dos Rios sample has undergone fluid-induced, retrograde metamorphism similar to the Tiburon sample.

3 Methods

3.1 Petrography

Examples of the four major mineral phases were identified using a petrographic microscope: omphacite, chlorite, phengite, and amphibole. Examples of the low-Li phases – titanite, epidote, and garnet – were also identified. The criteria for a grain to be included for analysis were: (i) relatively few inclusions; (ii) distinct grain boundaries in plane polarized light and in reflected light; and (iii) easy to distinguish mineral boundaries in both transmitted and reflected light. Grains were selected along traverses across the blueschist/eclogite interface in each sample to look for systematic changes in composition, and as a function of distance across the interface. More grains around the contact between blueschist and eclogite domains were chosen to attempt to identify the mm-scale features the infiltrating fluid may have left behind.

3.2 Electron Probe Microanalyzer (EPMA)

Major and minor element concentrations (Si, Ti, Al, Fe, Mn, Mg, Ca, Ba, Na, and K) of the phases were determined by a JEOL JXA-8900 Superprobe electron probe microanalyzer at the University of Maryland, College Park. Initial analysis consisted of confirmation of phase identities via energy dispersive spectrometry (EDS). Major and minor element analysis was accomplished via wavelength dispersive spectrometry (WDS). Minerals were analyzed using a beam potential or

accelerating voltage of 15 kV, a 5 μm spot size, and a 20 nA cup current. Count times of 10 – 60 s on peak and 5 – 30 s on background were used. Raw count rates were corrected using a ZAF algorithm to obtain concentrations. Table 3 has information on the standard reference materials that were used for the WDS analysis.

Phengite		Amphibole		Omphacite and Chlorite	
Element	Standards	Element	Standards	Element	Standards
Al	Garnet-12442	Al	Kakanui hornblende	Al	Garnet-12442
Ba	Orthoclase			Ca	Engels hornblende
Fe	Garnet-12442	Fe	Kakanui hornblende	Fe	Garnet-12442
K	Microcline	K	Kakanui hornblende	K	Orthoclase
Mg	Kakanui hornblende	Mg	Kakanui hornblende	Mg	Kakanui hornblende
Mn	Rhodonite	Mn	Rhodonite	Mn	Rhodonite
Na	Albite	Na	Kakanui hornblende	Na	Albite
Si	Staurolite	Si	Kakanui hornblende	Si	Staurolite
Ti	Kakanui hornblende	Ti	Kakanui hornblende	Ti	Kakanui hornblende

Table 3. Standards used in EPMA analyses.

3.3 Laser Ablation Inductively Coupled Mass Spectrometry (LA-ICP-MS)

The Li concentration in the phases was measured at the University of Maryland, College Park using a New Wave frequency-quintupled Nd-YAG laser (213 nm) coupled to a Thermo-Finnigan Element2 single collector ICP-MS with He flushing the ablation cell. Analyses were performed with a laser fluence of $\sim 2 - 3 \text{ Jcm}^{-2}$, a repetition rate of 7 Hz, and a spot size of 40 - 80 μm . The spot size used depended on the size of the mineral grain that was analyzed; the smaller minerals of any type required a smaller spot size. An analysis consisted of 15-20 s of background gathering, followed by 60 s of laser ablation. Analyses were performed in groups of

20 for ease of data reduction. Concentrations of B, Al, Ca, and Si were also analyzed. The first and last four analyses of each group were standard reference materials, BCR-2G and NIST 610. Data reduction was performed using LAMTRACE. Silicon was used as an internal standard to correct for ablation yields. The advantages of analyzing via LA-ICP-MS compared to methods such as solution are: 1) high precision, ng/g measurements; 2) little sample preparation; 3) small analytical blanks; 4) the ability to measure μm -sized samples with moderately little sample destruction; and 5) avoidance of surface and grain boundary contamination. Use of LA-ICP-MS allows for precise measurements of Li concentration in specific phases, instead of bulk portions of the rock. This will be useful to tell which phases Li preferentially partitions into, as well as the ability to measure small parts of mineral grains in context to the rest of the rock.

3.4 Error analyses

3.4.1 Point counting

The absolute 1σ uncertainty associated with counting mineral modes (refer to Tables 1 and 2) was calculated using the equation found in Van der Plas and Tobi (1965):

$$\sigma_i = \sqrt{\frac{p_i(100 - p_i)}{n}}$$

where p_i =volume percent mineral in a given rock and n is the total number of points counted. σ_i is the absolute uncertainty, in volume percent.

3.4.2 EPMA

The 1σ uncertainty is based on Poisson counting statistics on each analysis on the probe. The counting statistical error is calculated as $\sigma = \frac{1}{\sqrt{n}}$, where n = the number of x-ray counts collected by the EPMA. Each grain analyzed has 1-5 separate analyses per grain. For each element, the uncertainty for each grain was calculated by:

$$\sigma_m = \sqrt{\frac{\sum \sigma_{1-x}^2}{n}},$$

where σ_m is the standard deviation from the mean, $\sum \sigma_{1-x}^2$ is the sum of the squares of all the errors of the analyses of a grain, and n is the number of analyses. This process is repeated for each element analysis of a grain. BSE imaging revealed that some omphacite, phengite, and amphibole grains are zoned. No zones are large enough to be analyzed by LA-ICP-MS (smaller than 20 μm in diameter), so no special protocol was followed to account for zonation.

3.4.3 LA-ICP-MS

The 1σ uncertainty is based on Poisson counting statistics on each analysis on the laser. Each calculation is based upon the number of counts of Li given by the MS. The counting statistical error for each analysis is calculated as: $\sigma = \frac{1}{\sqrt{tc}}$, where t = time, in seconds, of ablation; and c = counts of ^7Li per second. ^7Li is the preferred isotope for error analysis, as ^7Li represents 92.5% of natural Li and thus produces many more counts during ablation. The greater number of counts will produce a smaller σ for each analysis.

3.4.4 Error propagation

Each mineral grain was analyzed 1-5 times. The Li concentration of each grain is the average of all Li concentrations of the analyses of a grain. The uncertainty of the Li concentration for each grain is calculated by averaging the error per analysis using the standard deviation from the mean: $\sigma_m = \sqrt{\frac{\sum \sigma_{1-x}^2}{n}}$, where $\sum \sigma_{1-x}^2$ is the sum of the squares of all the errors of the analyses of a grain, and n = the number of analyses. The uncertainty of eclogite and blueschist is calculated as the standard deviation of the Li concentration of the population. The statistical difference between populations was determined using t-tests. A two-tailed, unpaired t-test was performed on each population of analyses. If the populations had a similar standard deviation, a standard unpaired t-test was used; if the standard deviations were different, Welsh's t-test was performed. P-values of 0.05 or less were considered statistically significant (Ruxton, 2006).

The total uncertainty for each analysis is based on the total uncertainty from the counting statistics on each LA-ICP-MS measurement, the EPMA uncertainty on the internal standard measurement, and the systematic error on BCR2g. The total uncertainty on an analysis is calculated as:

$$\sqrt{\left(\frac{S_a}{a}\right)^2 + \left(\frac{S_b}{b}\right)^2 + \left(\frac{S_c}{c}\right)^2}$$

where $\left(\frac{S_a}{a}\right)^2$ is the uncertainty from the Poisson counting statistics from the Li concentration measurements on the LA-ICP-MS, $\left(\frac{S_b}{b}\right)^2$ is the uncertainty from the

EPMA, and $\left(\frac{s_c}{c}\right)^2$ is the standard deviation of the standard reference material BCR2g.

The 1σ standard deviation on 22 analyses of ^7Li is 6.9% and the $1\sigma_{\text{mean}}$ is 1.5%. The accuracy of BCR2g is 5.8% at 9.6 $\mu\text{g/g}$ Li using the preferred GeoReM value of 9 ± 1 $\mu\text{g/g}$. NIST610 was also measured, but not used for error propagation due to its much different Li concentration from the samples in this study. The 1σ standard deviation for 24 analyses of NIST610 is 1.4% and the $1\sigma_{\text{mean}}$ is 0.3%.

4 Results

Minerals of interest (i.e., grains with well-defined grain boundaries and no apparent grain overlap) were identified using petrographic microscope and their identities confirmed using qualitative EDS analysis. Major and minor element concentrations were determined using quantitative WDS analysis. Those minerals were then subsequently analyzed via LA-ICP-MS to determine their Li concentration. Amphibole, omphacite, phengite, and chlorite in eclogite and blueschist domains were analyzed in the Tiburon sample. Amphibole, omphacite, and phengite were analyzed in both domains in the Dos Rios sample. In addition, minor lithium-bearing phases (garnet, titanite, and epidote) were analyzed in both samples.

4.1 Textural observations

4.1.1 Tiburon

The Tiburon sample has textural evidence of fluid-mediated retrograde metamorphism. The Tiburon sample has garnets in the eclogitic domain, grading to partially chloritized garnets within the blueschist adjacent to the eclogite/blueschist contact, to fully chloritized garnet pseudomorphs farther away from the contact in the

blueschist domain (Figure 6). Given chlorite is interpreted as forming during retrograde metamorphism and chlorite is a hydrous phase, then these pseudomorphs are indicators of fluid-rock interaction. Pumpellyite is another hydrous phase found only in the blueschist domain of the Tiburon sample. Pumpellyite is stable at temperatures lower than the peak metamorphic assemblage found in the eclogite layer (Liou et al., 1987). Further evidence of fluid-rock interaction is apparent in backscattered electron (BSE) images of the omphacites in the Tiburon sample. Omphacites from the eclogite domain appear to be relatively homogeneous with some zoning that is likely growth zoning on the rims. Approaching the contact and into the blueschist layer, omphacites are mostly homogeneous but have some light-colored, Ca-rich (i.e., more diopsidic rather than jadeitic, in some places replaced by pumpellyite) patches (Figure 4). Further into the blueschist layer, away from the contact, the omphacites have more of these Ca-rich patches.

4.1.2 Dos Rios

In contrast, the Dos Rios sample has no textural evidence of fluid-mediated retrograde metamorphism. Both the eclogite and blueschist domains have, compared to the Tiburon sample, unaltered garnets (see Figure 3). Pumpellyite is not a phase that is seen in either the blueschist or the eclogite domain in the Dos Rios sample. Finally, BSE imaging of omphacites in the Dos Rios sample shows no patchy, Ca-rich regions in omphacites.

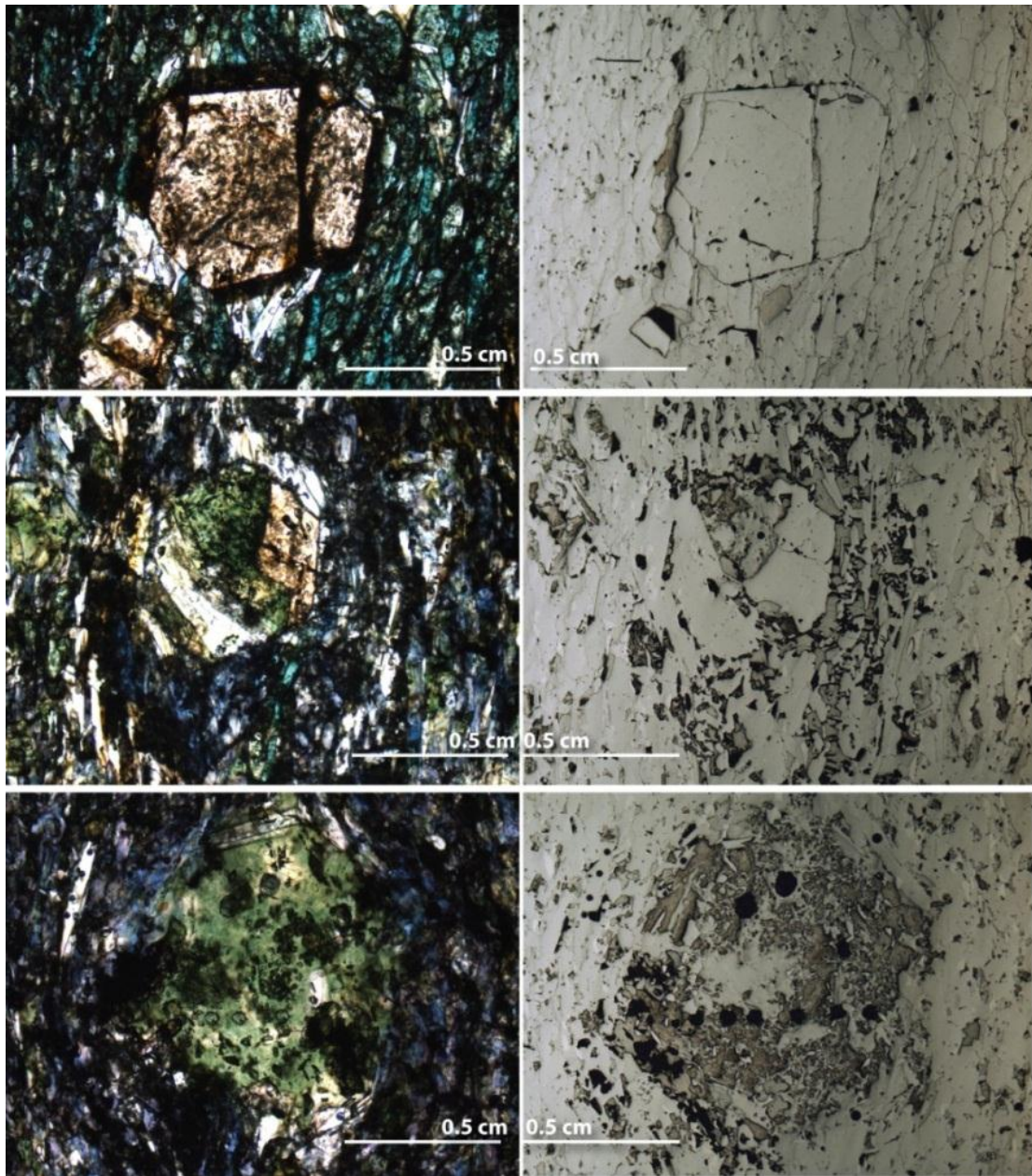


Figure 6. Plane polarized light (images in left column) and reflected light (images in right column) photomicrographs of garnets in Tiburon sample, showing gradation to chlorite pseudomorphs farther away from the eclogite/blueschist boundary. The top two photos are of unaltered garnets 1 cm away from the eclogite/blueschist contact in the eclogite domain. The center two photos are of partially chloritized garnets 1 cm away from the contact in the blueschist domain. The bottom two photos are completely chloritized garnets 2 cm away from the contact in the blueschist domain.

4.2 EPMA Results

4.2.1 Amphibole

Tiburon amphiboles comprise about 13% of the volume of the eclogite and about 47% of the volume of the blueschist. In the eclogite, the average amphibole formula is $\text{Na}_{0.2}(\text{Na}_{1.7}\text{Fe}_{0.2}\text{Ca}_{0.2})(\text{Mg}_{2.1}\text{Fe}_{1.3}\text{Al}_{1.7})(\text{Si}_{7.8}\text{Al}_{0.2})\text{O}_{22}(\text{OH})_2$. In the blueschist, the average amphibole formula is $\text{Na}_{0.2}(\text{Na}_{1.7}\text{Fe}_{0.1}\text{Ca}_{0.2})(\text{Mg}_{2.2}\text{Fe}_{1.2}\text{Al}_{1.6})(\text{Si}_{7.8}\text{Al}_{0.2})\text{O}_{22}(\text{OH})_2$. Refer to Figure 7 for a graphical representation of the amphibole compositions. All but one of the amphibole compositions fall within the compositional range for glaucophane (Hawthorne and Oberti, 2007). That anomalous amphibole has slightly less Na and classifies as winchite. The composition of the Tiburon amphiboles from the eclogite and blueschist domains are similar.

Dos Rios amphiboles comprise about 15% of the volume of the eclogite and about 47% of the volume of the blueschist. In the eclogite, the average amphibole formula is $\text{Na}_{0.2}(\text{Na}_{1.6}\text{Fe}_{0.2}\text{Ca}_{0.2})(\text{Mg}_{2.0}\text{Fe}_{1.4}\text{Al}_{1.6})(\text{Si}_{7.9}\text{Al}_{0.1})\text{O}_{22}(\text{OH})_2$. In the blueschist, the average amphibole formula is $\text{Na}_{0.2}(\text{Na}_{1.6}\text{Fe}_{0.2}\text{Ca}_{0.2})(\text{Mg}_{1.9}\text{Fe}_{1.5}\text{Al}_{1.6})(\text{Si}_{7.9}\text{Al}_{0.1})\text{O}_{22}(\text{OH})_2$. Refer to Figure 7 for a graphical representation of the amphibole compositions. All but one of the amphibole compositions fall within the range for glaucophane (Hawthorne and Oberti, 2007). That anomalous amphibole has slightly less Na and classifies as winchite. The composition of the Dos Rios amphiboles from the eclogite and blueschist domains are similar. Compared to the Tiburon amphiboles, the Dos Rios amphiboles have slightly more Si, slightly more Fe, and slightly less Mg.

		Amphibole						Omphacite			
		Eclogite		Blueschist				Eclogite		Blueschist	
		avg. wt%	σ	avg. wt%	σ			avg. wt%	σ	avg. wt%	σ
SiO ₂		56.8	0.5	56.7		SiO ₂		55.1	0.7	54.7	0.7
TiO ₂		bd		bd	0.3	TiO ₂		bd			
Al ₂ O ₃		11.3	0.4	11.0	0.8	Al ₂ O ₃		10.0	0.5	8.7	1.5
FeO		11.7	0.6	11.8	1.2	FeO		7.6	0.7	8.6	1.0
MnO		bd		bd		MnO		bd	bd		
MgO		10.0	0.5	10.2	1.2	MgO		7.2	0.4	7.6	0.4
CaO		1.7		1.8	0.6	CaO		13.5	0.6	14.1	1.1
BaO		bd				BaO		bd		bd	
Na ₂ O		6.9	0.6	6.7	0.3	Na ₂ O		6.2	0.3	6.1	0.6
K ₂ O		bd	bd	bd		K ₂ O		bd		bd	
Total		98.3	0.5	98.3	0.5	Total		100	0.9	100	1.0
No. analyses		8		18		No. analyses		14		9	
		Phengite						Chlorite			
		Eclogite		Blueschist				Eclogite		Blueschist	
		avg. wt%	σ	avg. wt%	σ			avg. wt%	σ	avg. wt%	σ
SiO ₂		49.6	0.5	50.2	0.7	SiO ₂		27.9	0.4	28.5	0.4
TiO ₂						TiO ₂		bd		bd	
Al ₂ O ₃		28.2	0.5	27.7	0.7	Al ₂ O ₃		18.4	0.5	18.6	0.5
FeO		2.5	0.1	2.5	0.2	FeO		27.2	2.2	24.2	1.90
MnO		bd				MnO		bd		bd	
MgO		2.9	0.2	3.1	0.2	MgO		14.1	1.7	17.0	1.4
CaO		bd		bd		CaO		bd		bd	
BaO		bd		bd		BaO		bd		bd	
Na ₂ O		0.9	0.1	0.8	0.2	Na ₂ O		bd		bd	
K ₂ O		10.1	0.3	10.30	0.3	K ₂ O		bd		bd	
Total		94.2	0.4	94.6	0.5	Total		88.8	0.8	88.6	
No. analyses		10		17		No. analyses		17		23	

Table 3. EPMA results for major Li-bearing phases in the Tiburon sample.

		Amphibole						Omphacite			
		Eclogite		Blueschist				Eclogite		Blueschist	
		avg. wt%	σ	avg. wt%	σ			avg. wt%	σ	avg. wt%	σ
SiO ₂		56.2	0.6	56.4	0.4	SiO ₂		54.7	0.3	54.5	0.3
TiO ₂		bd		bd		TiO ₂		bd			
Al ₂ O ₃		9.9	0.6	10.3	0.4	Al ₂ O ₃		7.5	0.6	7.4	1.0
FeO		13.3	1.3	12.5	0.7	FeO		8.7	0.5	9.1	0.8
MnO		bd		bd		MnO		bd			
MgO		9.3	0.7	9.8	0.4	MgO		7.7	0.5	7.6	0.5
CaO		1.2	0.5	1.1	0.2	CaO		13.5	0.6	13.4	0.8
BaO		bd		bd		BaO		bd		bd	
Na ₂ O		6.8	0.4	7.0	0.2	Na ₂ O		7.0	0.4	7.0	0.4
K ₂ O		bd	bd	bd	bd	K ₂ O		bd		bd	
Total		96.9	0.4	97.1	0.4	Total		99.2	0.5	99.2	0.3
No. analyses		10		11		No. analyses		11		11	
		Phengite									
		Eclogite		Blueschist							
		avg. wt%	σ	avg. wt%	σ						
SiO ₂		51.7	0.5	51.8	0.9						
TiO ₂		bd		bd							
Al ₂ O ₃		24.8	0.8	24.8	0.8						
FeO		3.5	0.4	3.5	0.4						
MnO		bd		bd							
MgO		3.9	0.2	3.9	0.2						
CaO		bd		bd							
BaO		bd		bd							
Na ₂ O		0.2	0.1	0.2	0.1						
K ₂ O		10.7	0.8	10.7	0.8						
Total		94.9	0.8	94.9	0.8						
No. analyses		11		8							

Table 4. EPMA results for major Li-bearing phases in the Tiburon sample.

4.2.2 Omphacite

Tiburón omphacites comprise about 39% of the volume of the eclogite and about 8.9% of the volume of the blueschist. In the eclogite, the average omphacite formula is $(\text{Na}_{0.4}\text{Ca}_{0.5})(\text{Fe}_{0.2}\text{Mg}_{0.4}\text{Al}_{0.4})\text{Si}_{1.9}\text{O}_6$. For the omphacites in the blueschist, only the Na-rich portions of the omphacite were measured, not the Ca-rich patches. In the blueschist, the average omphacite formula is $(\text{Na}_{0.4}\text{Ca}_{0.5})(\text{Fe}_{0.3}\text{Mg}_{0.4}\text{Al}_{0.4})\text{Si}_{1.8}\text{O}_6$. The omphacite compositions are plotted in Figure 8, where %Jadite is the NaAl pyroxene endmember, %Diopside-Hedenbergite is the $\text{Ca}(\text{Fe}^{2+}, \text{Mg})$ endmember, and %Acmite is the Fe^{3+} endmember. The omphacites are homogeneous in composition, as they cluster together in one portion of the quadrilateral. The Fe and Mg content of the omphacites do not vary between eclogite and blueschist domains.

Dos Rios omphacites comprise about 33% of the volume of the eclogite and about 4% of the volume of the blueschist. In the eclogite, the average omphacite formula is $(\text{Na}_{0.5}\text{Ca}_{0.5})(\text{Fe}_{0.3}\text{Mg}_{0.4}\text{Al}_{0.3})\text{Si}_{2.0}\text{O}_6$; in the blueschist, the average omphacite formula is $(\text{Na}_{0.5}\text{Ca}_{0.5})(\text{Fe}_{0.3}\text{Mg}_{0.4}\text{Al}_{0.3})\text{Si}_{2.0}\text{O}_6$. The Dos Rios omphacites are, like their Tiburón counterparts, generally homogeneous in composition. The Fe and Mg content of omphacites from eclogite and blueschist domains are similar.

The omphacites in the Dos Rios sample have a restricted compositional range when compared to the Tiburón sample. Both samples are homogeneous; that is, the omphacites in both samples have similar %Al, %Ca, and % Fe^{3+} components. The Dos Rios sample has greater %Ca and less % Fe^{3+} components than the Tiburón sample.

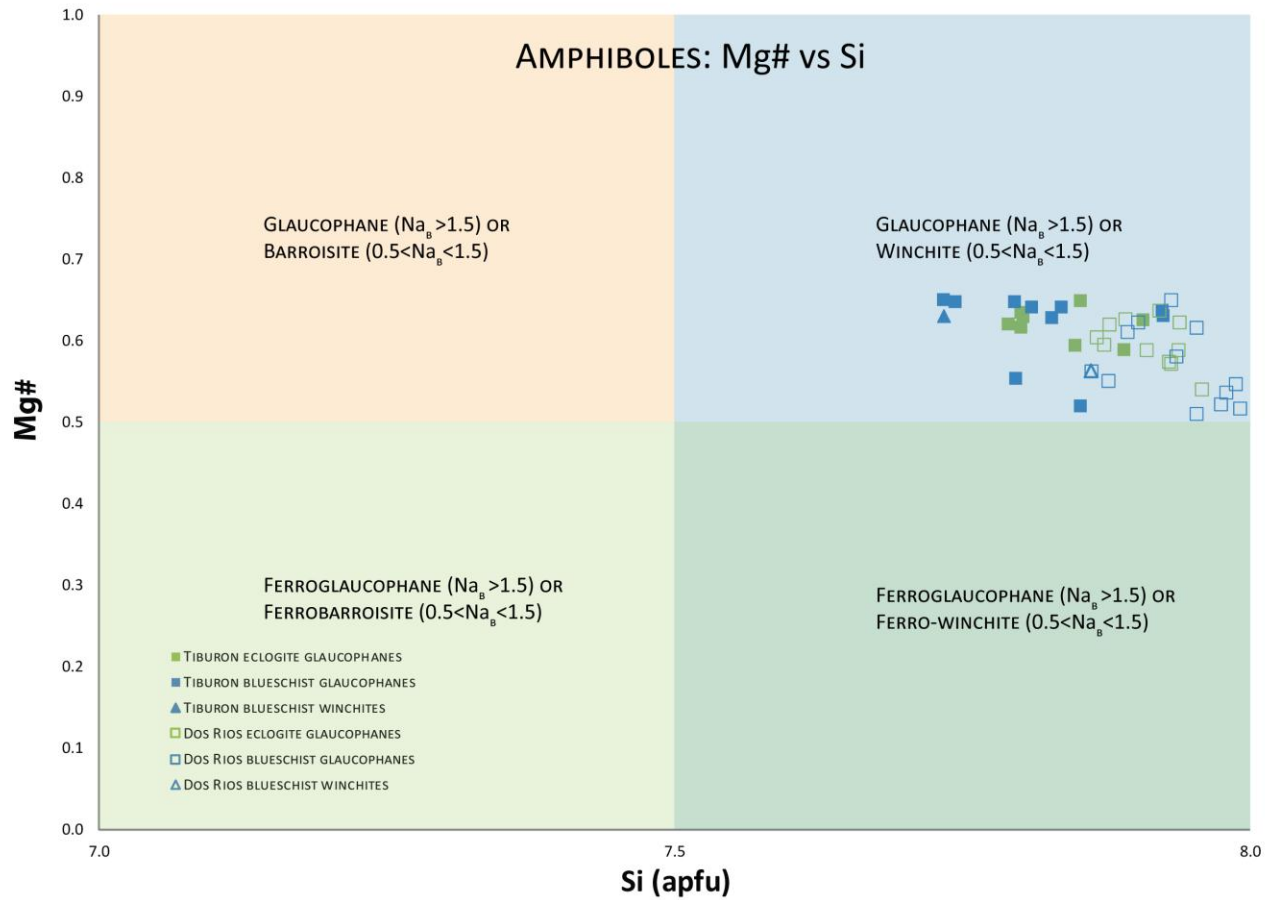


Figure 7. Diagram showing the distribution of amphibole compositions in the Tiburon and Dos Rios sample, where Mg# is $(Mg+Fe)/Mg$ and Mg and Fe are measured in atoms per formula unit (apfu), and Si is measured in apfu. Subscript B represents Na in octahedral site. All of the amphiboles fall within the compositional range for a glaucophane or winchite, depending on their Na composition. Amphibole composition scheme after (Hawthorne and Oberti, 2007).

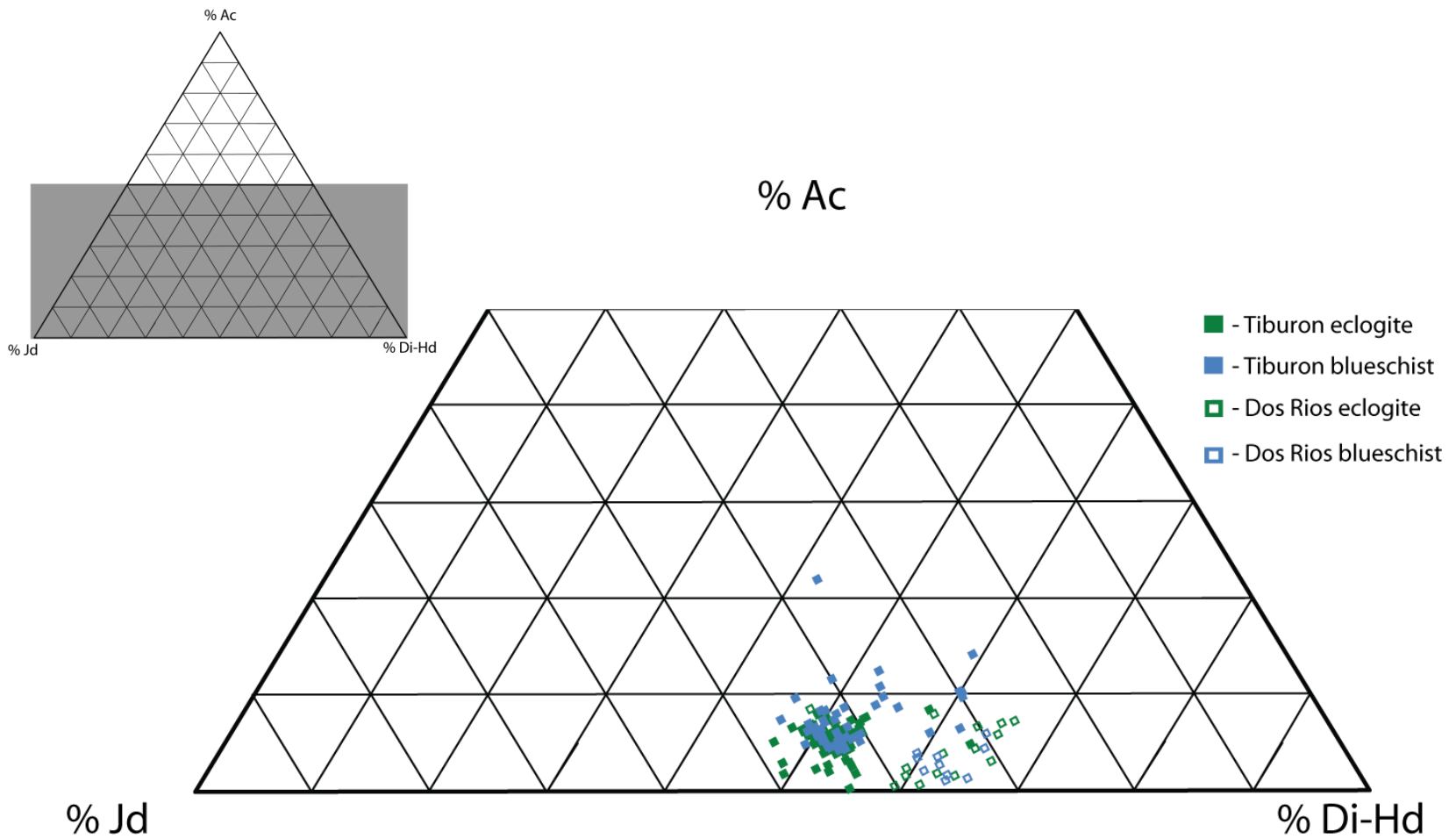


Figure 8. Quadrilateral diagram showing the composition of omphacites in the Tiburon and Dos Rios samples. Jd=Jadeite; Di-Hd= Diopside-Hedenbergite; Ac=Acmite. The omphacites mostly cluster between 40 % Jd and 55 % Di-Hd for the Tiburon sample and 30% Jd and 65% DiHd for the Dos Rios samples. The Tiburon and Dos Rios samples have distinct omphacite compositions. The average pyroxene composition is 39% Jd, 54% Di-Hd, 7% Ac for the Tiburon sample and 31% Jd, 66% Di-Hd, and 3% Ac for the Dos Rios sample.

4.2.3 Phengite

4.2.3.1 Tiburon phengites

Tiburon phengites comprise about 18% of the volume of the eclogite and about 20% of the blueschist. In the eclogite, the average phengite formula is $(K_{0.9}Na_{0.1})(Fe_{0.2}Mg_{0.3}Al_{1.5})(Al_{0.7}Si_{3.3})O_{10}(OH)_2$. In the blueschist, the average phengite formula is $(K_{0.8}Na_{0.1})(Fe_{0.2}Mg_{0.4}Al_{1.5})(Al_{0.6}Si_{3.4})O_{10}(OH)_2$. These mineral formulae are similar to the ones calculated in the same sample in Sorensen et al. (1997). In that study, the average phengite formula was $(K_{0.9}Na_{0.1})(Fe_{0.2}Mg_{0.3}Al_{1.5})(Al_{0.6}Si_{3.4})O_{10}(OH)_2$ in the eclogite domain and $(K_{0.9}Na_{0.1})(Fe_{0.2}Mg_{0.3}Al_{1.5})(Al_{0.7}Si_{3.4})O_{10}(OH)_2$ in the blueschist domain.

All of the compositions of phengite fall below the line for an idealized Tschermak substitution (e.g., $MgSi \rightleftharpoons Al_{VI}Al_{IV}$), meaning that the phengite compositions are dominated by Tschermak substitution (Figure 9). The eclogite and blueschist phengite compositions mostly overlap – there are no systematic changes between phengite compositions going from eclogite to blueschist domains. There is some variability in phengite compositions across the sample (ranging from 3.3 to 3.45 atoms per formula unit), although this variability is not systematic going from eclogite to blueschist. These phengites have a similar Mg. vs. Si trend as in Sorensen et al. (1997), which analyzed phengites from the same locality.

The phengite compositions in the Tiburon sample have variable paragonite content; i.e., the Na concentration ranges from 0.05 to 0.15 apfu (Figure 10). There is no systematic change in paragonite content going from eclogite to blueschist domains), and the phengites in the blueschist domain tend to have a higher phengite

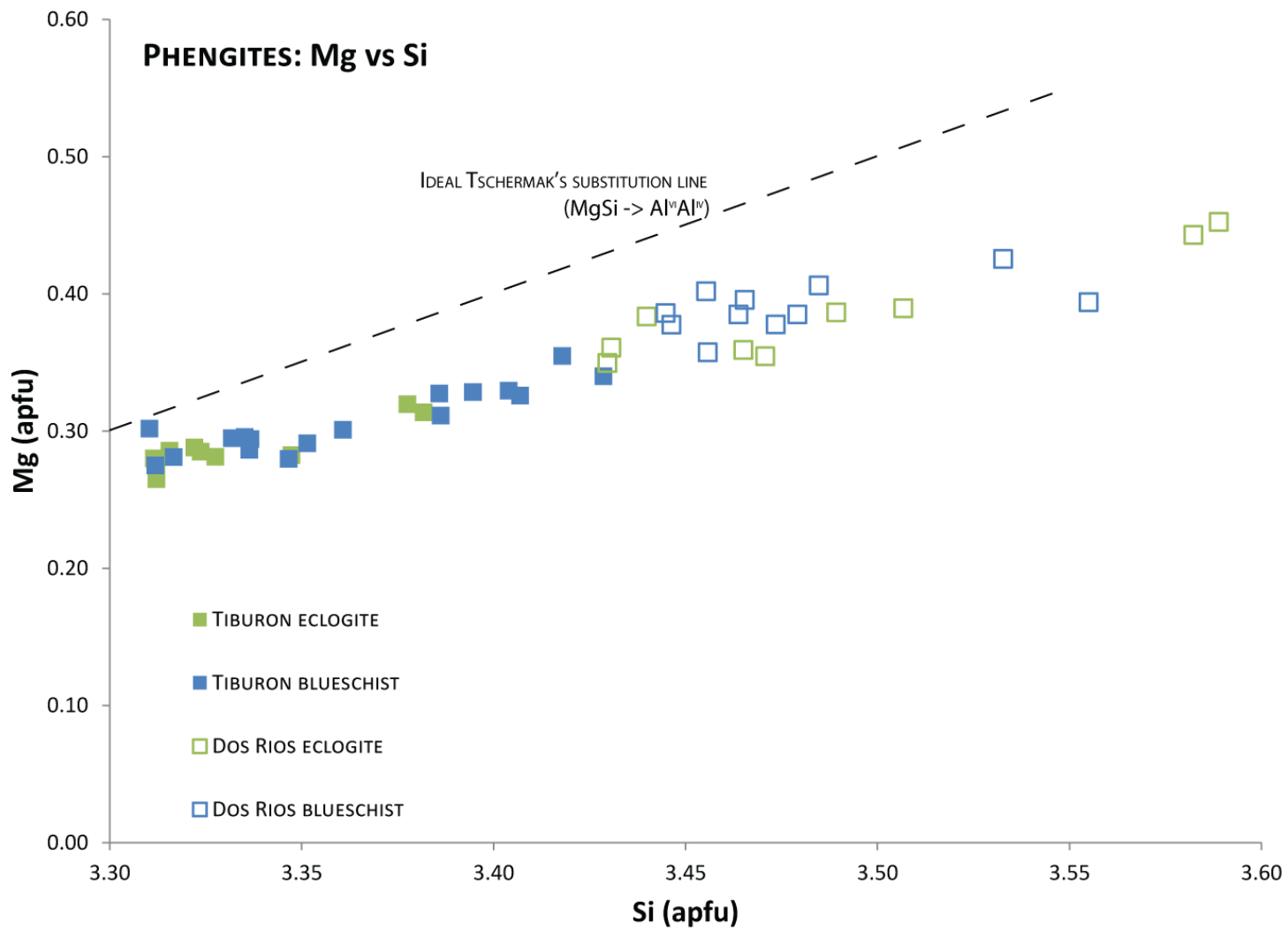


Figure 9. Mg vs Si concentrations of Tiburon (closed symbols) and Dos Rios (open symbols) phengites. All of the phengites fall below the line representing an perfect MgSi – AlAl substitution.

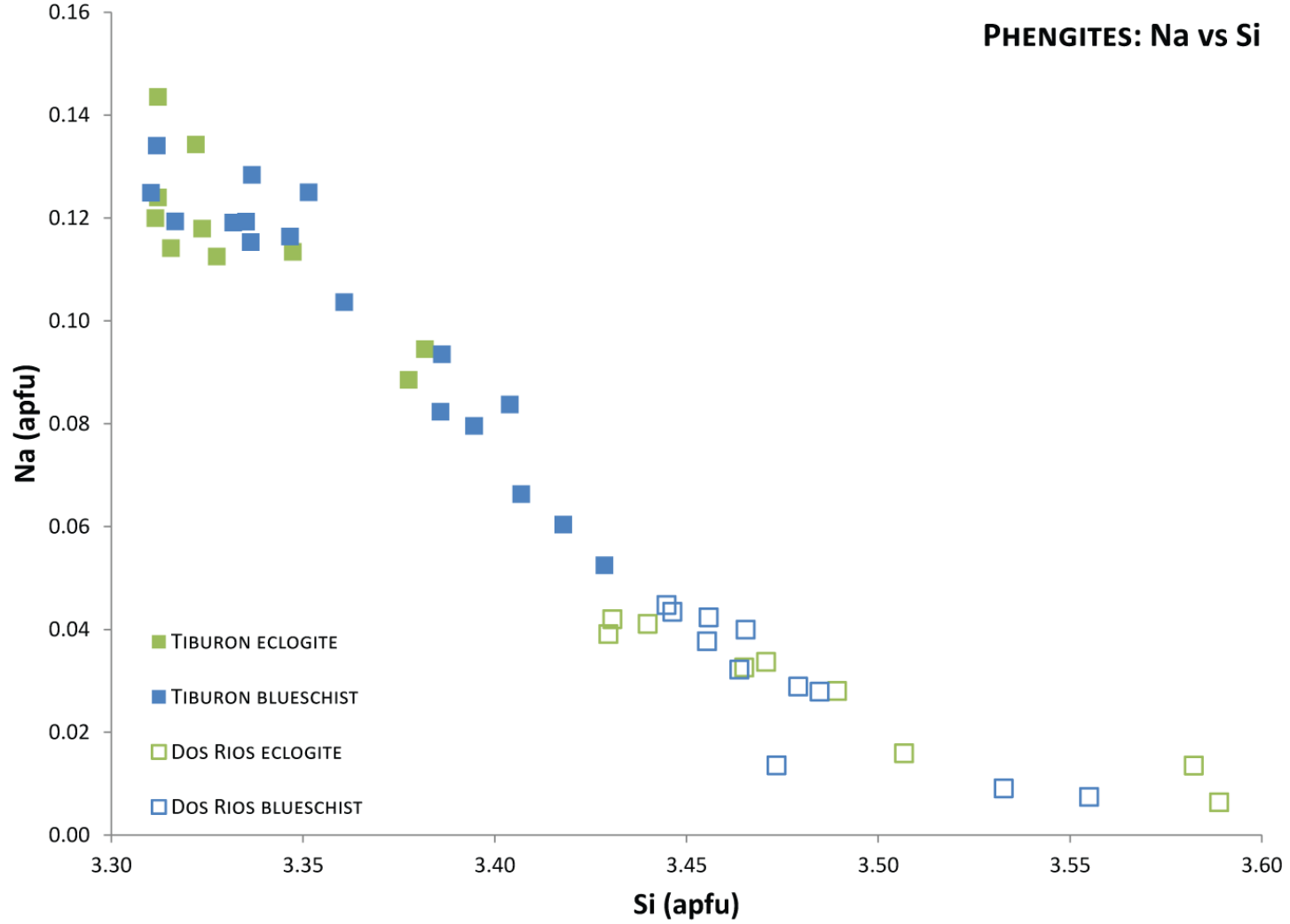


Figure 10. Na vs Si concentrations of Tiburon (closed symbols) and Dos Rios (open symbols) phengites. The phengites in the Tiburon sample tend to have a higher paragonite component (i.e., higher in Na composition), than the phengites in the Dos Rios sample.

component (i.e., lower in Na composition). Phengites with a relatively high paragonite content (about 0.12 apfu, similar to the phengites in the Tiburon eclogite domain) are generally found in rocks that have experienced moderate to high-T subduction zone metamorphic conditions (Sorensen et al., 1997 and references therein). Phengites with lower paragonite content – similar to many of the phengites in the blueschist domain in the Tiburon sample – are correlated with late retrograde crystallization of phengite. Thus, the paragonite content of phengite in the blueschist reflects the period in the metamorphic history that it crystallized (Sorensen et al., 1997). Phengites that crystallized earlier are expected to have similar paragonite content as those in the eclogite domain, but phengites that crystallized later are expected to have lower paragonite contents when compared to those in the eclogite domain.

4.2.3.2 Dos Rios phengites

Dos Rios phengites comprise about 12% of the volume of the eclogite and 1.7% of the volume of the blueschist. In the eclogite, the average phengite formula is $K_{0.9}(Fe_{0.2}Mg_{0.4}Al_{1.4})(Al_{0.5}Si_{3.5})O_{10}(OH)_2$. In the blueschist, the average phengite formula is $K_{0.9}(Fe_{0.2}Mg_{0.4}Al_{1.4})(Al_{0.5}Si_{3.5})O_{10}(OH)_2$. These phengite formulas are similar to the average phengite formula calculated for the same sample in Sorensen et al. (1997) – $K_{0.9}Na_{0.1}(Fe_{0.2}Mg_{0.4}Al_{1.4})(Al_{0.6}Si_{3.4})O_{10}(OH)_2$. However, the phengites in the Sorensen et al. (1997) study have a higher Na content than the phengites analyzed in this study.

Figure 9 shows that all compositions of Dos Rios phengites fall below the line for an idealized Tschermak substitution. This means that the phengite compositions in

the Tiburon sample are dominated by Tschermak substitution. The phengites analyzed in the Dos Rios sample in this study follow a similar Mg. vs. Si trend as in Sorensen et al. (1997), which found that the phengites were also defined by Tschermak substitution. There is some variability in phengite compositions across the sample (ranging from 3.45 to 3.60 atoms per formula unit), although this variability is not systematic going from eclogite to blueschist. As with the Tiburon phengites, these Dos Rios phengites have a similar Mg. vs. Si trend as in Sorensen et al. (1997).

The Na content in the Dos Rios sample is lower than in the Tiburon sample (Figure 10). Similar compositions were observed in phengites analyzed in Sorensen et al. (1997). The phengite compositions that are above the detection limit for Na (~0.02 apfu Na) all cluster together, not in distinct compositional regimes as in the Tiburon sample. The Dos Rios phengites also have a higher Si content than the Tiburon phengites.

4.2.4 Chlorite

In the Tiburon sample, the chlorites comprise about 3.3% of the volume of the eclogite and about 9.7% of the volume of the blueschist. In the eclogite, the average chlorite formula is $(\text{Fe}_{2.4} \text{Mg}_{2.2} \text{Al}_{1.4})(\text{Al}_{0.9} \text{Si}_{2.9})\text{O}_{10}(\text{OH})_8$. In the blueschist, the average chlorite formula is $(\text{Fe}_{2.1} \text{Mg}_{2.6} \text{Al}_{1.3})(\text{Al}_{1.0} \text{Si}_{2.9})\text{O}_{10}(\text{OH})_8$. The average chlorite formula falls in the solid solution series between the Mg-rich endmember, clinocllore, and the the Fe^{2+} -rich endmember, chamosite. The eclogite chlorites have a slightly higher chamosite component than the chlorites in the blueschist domain. The Al and Si components are about the same for the Tiburon chlorites in both domains. The Fe/Mg ratio decreases in a linear fashion ($R^2=0.6$) traversing across the

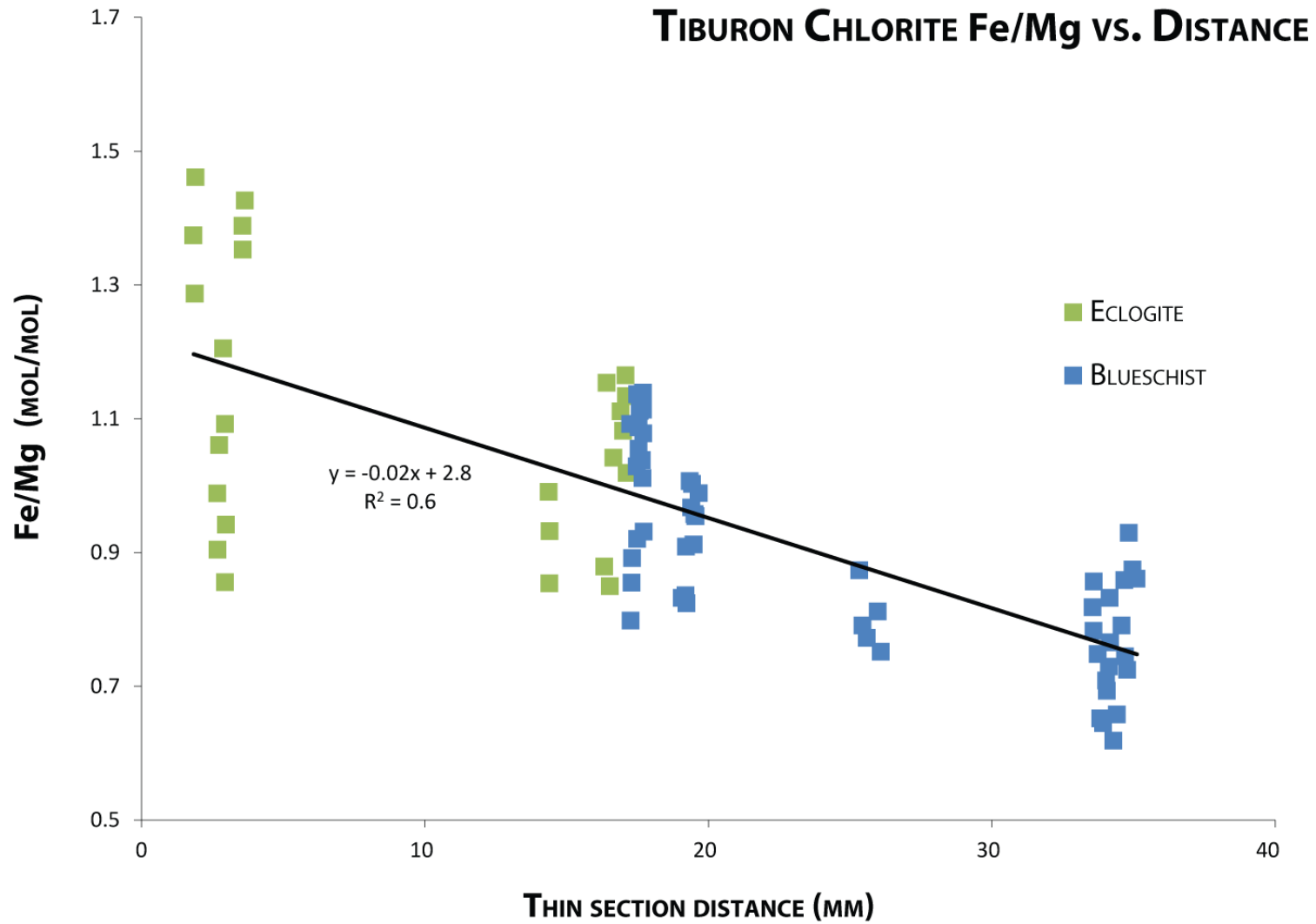


Figure 11. The Fe/Mg ratio in chlorites going horizontally along a traverse across the Tiburon sample, based on EPMA results. The ratio decreases from the eclogite to the blueschist portion of the sample

Tiburon sample from eclogite to blueschist (Figure 11). The significance of this trend is unclear. There is not a significant amount of chlorite in the Dos Rios sample (refer to Table 2), so a chlorite formula is not presented.

4.2.5 Low-Li phases

In the Tiburon sample, the average garnet formula is $(\text{Ca}_{0.9}\text{Fe}_{1.7}\text{Mg}_{0.3}\text{Mn}_{0.2})\text{Al}_{2.0}\text{Si}_{3.0}\text{O}_{12}$, the average titanite formula is $\text{Ca}_{0.9}(\text{Al}_{0.1}\text{Ti}_{1.0})\text{Si}_{1.1}\text{O}_5$, and the average epidote formula is $\text{Ca}_{2.1}(\text{Al}_{2.4}\text{Fe}_{0.6})\text{Si}_{3.1}\text{O}_{12}(\text{OH})$. In the Dos Rios sample, the average garnet formula is $(\text{Ca}_{0.9}\text{Fe}_{1.8}\text{Mg}_{0.2}\text{Mn}_{0.2})\text{Al}_{2.0}\text{Si}_{3.0}\text{O}_{12}$, the average titanite formula is $\text{Ca}_{1.1}(\text{Al}_{0.1}\text{Ti}_{0.9})\text{Si}_{1.1}\text{O}_5$, and the average epidote formula is $\text{Ca}_{2.0}(\text{Al}_{2.3}\text{Fe}_{0.7})\text{Si}_{3.1}\text{O}_{12}(\text{OH})$.

4.3 LA-ICP-MS Results

All Li concentration results are represented by box and whisker plots. For $n < 4$ in the bin of analyses, the boxes show the Li concentration of that sample and its spatial location in the sample. For $n > 4$ for the bin, the yellow line within the box indicates the median of the data and the horizontal whisker intersects the box at the mean of the data. The top vertical whisker represents the highest extent of data within 1.5 interquartile range (abbreviated IQR, where $\text{IQR} = 3^{\text{rd}} \text{ quartile} - 1^{\text{st}} \text{ quartile}$) of the upper quartile and the bottom whisker represents the lowest extent of data within 1.5 IQR of the lower quartile. The crosses indicate outliers outside of 1.5 IQR of the upper or lower quartile.

4.3.1 Amphibole

Tiburon amphiboles have an average Li concentration of 20 ± 4.7 (1σ) $\mu\text{g/g}$ in the eclogite portion of the sample and 16 ± 3.6 $\mu\text{g/g}$ in the blueschist portion of the sample (Figure 12). A t-test was performed on the two Li concentration populations and yielded a p-value of 0.04, indicating the difference between eclogite and blueschist is statistically significant. Dos Rios amphiboles have an average Li concentration 30 ± 3.1 $\mu\text{g/g}$ in the eclogite portion of the sample and 31 ± 5.1 $\mu\text{g/g}$ in the blueschist portion of the rock (Figure 13). A t-test performed on the two Li concentration populations and yielded a value of 0.6, indicating that the difference between eclogite and blueschist is not statistically significant. The Li concentration of amphiboles is higher in the Dos Rios sample than in the Tiburon sample.

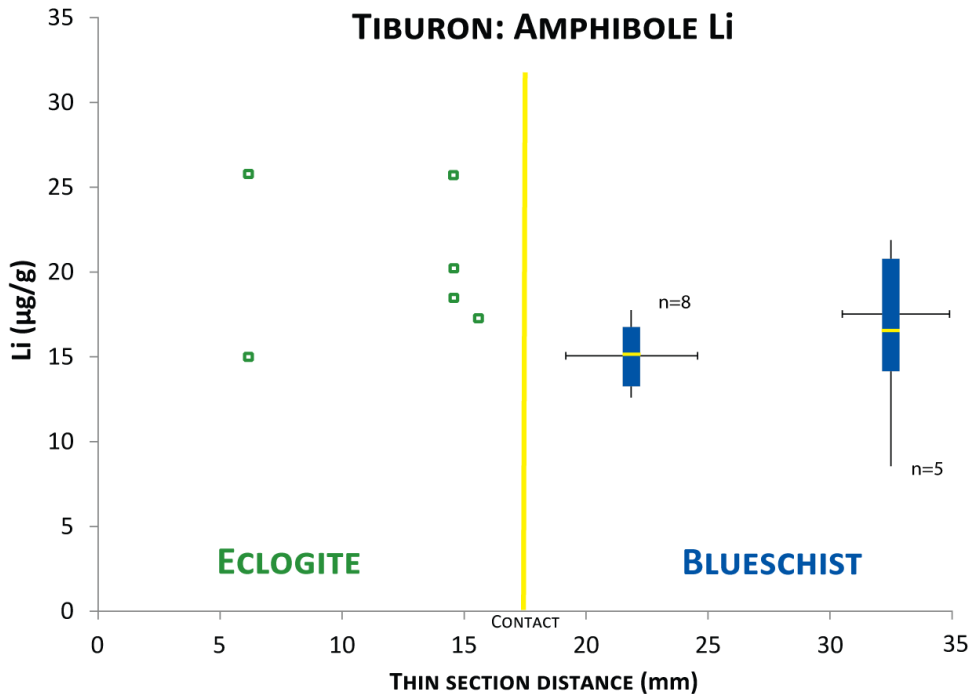


Figure 12. Tiburon amphibole Li concentrations.

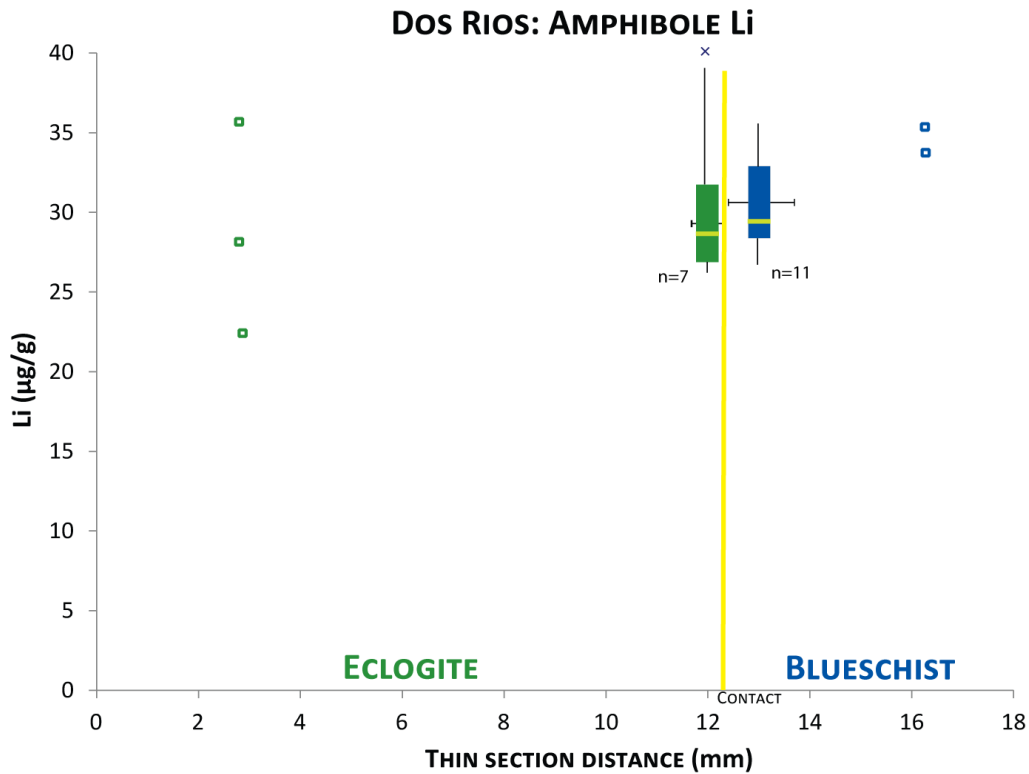


Figure 13. Dos Rios amphibole Li concentrations.

4.3.2 Omphacite

Tiburón omphacites have an average Li concentration of omphacites is 56 ± 11 $\mu\text{g/g}$ in the eclogite portion of the sample and 33 ± 21 $\mu\text{g/g}$ in the blueschist portion of the sample (Figure 14). For the omphacite in the Tiburón sample, the average Li concentration is higher in the eclogite domain than in the blueschist domain; the t-test yielded a p-value of 0.004, indicating that this difference is statistically significant. Dos Rios omphacites have an average Li concentration of 46 ± 3.9 $\mu\text{g/g}$ in the eclogite portion of the sample and 37 ± 8.1 $\mu\text{g/g}$ in the blueschist portion of the sample (Figure 15). In the Dos Rios sample, there is a statistically significant difference between omphacites in the eclogite and blueschist domains. The Li concentration of omphacites in the eclogite is higher in the Tiburón sample than in the

Dos Rios sample; the t-test yielded a p-value of 0.01 for the two populations, so this difference is statistically significant.

4.3.3 Phengite

Tiburón phengites have an average Li concentration of phengites is 37 ± 2.2 $\mu\text{g/g}$ in the eclogite portion of the sample and 33 ± 6.8 $\mu\text{g/g}$ in the blueschist portion of the sample (Figure 16). The t-test yielded a p-value of 0.07, indicating that the difference between eclogite and blueschist domains are not statistically significant.

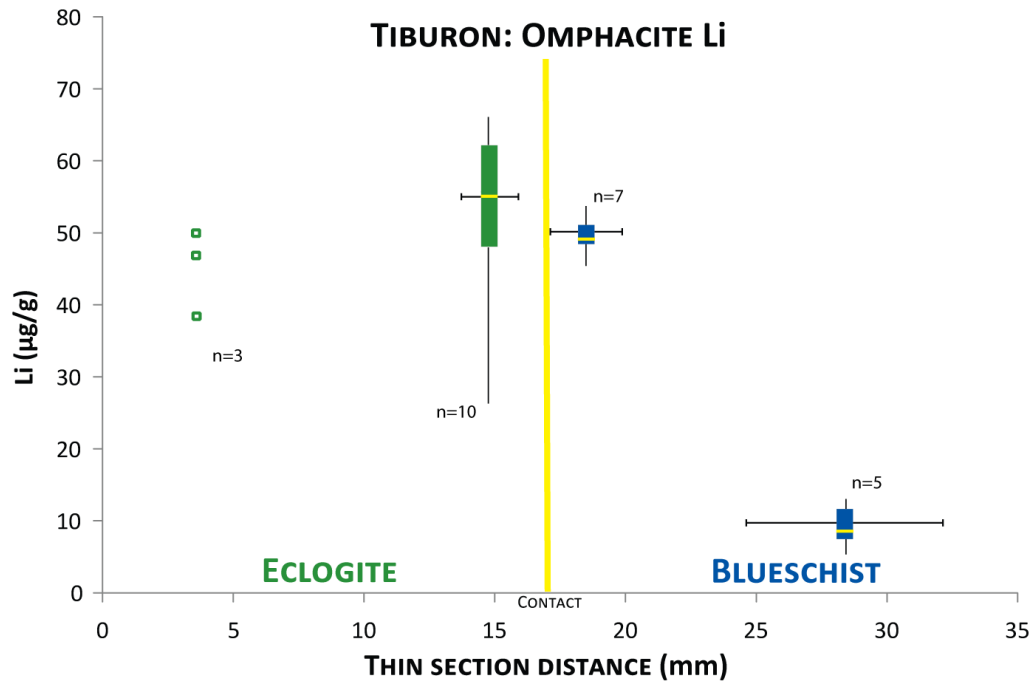


Figure 14. Tiburón omphacite Li concentrations.

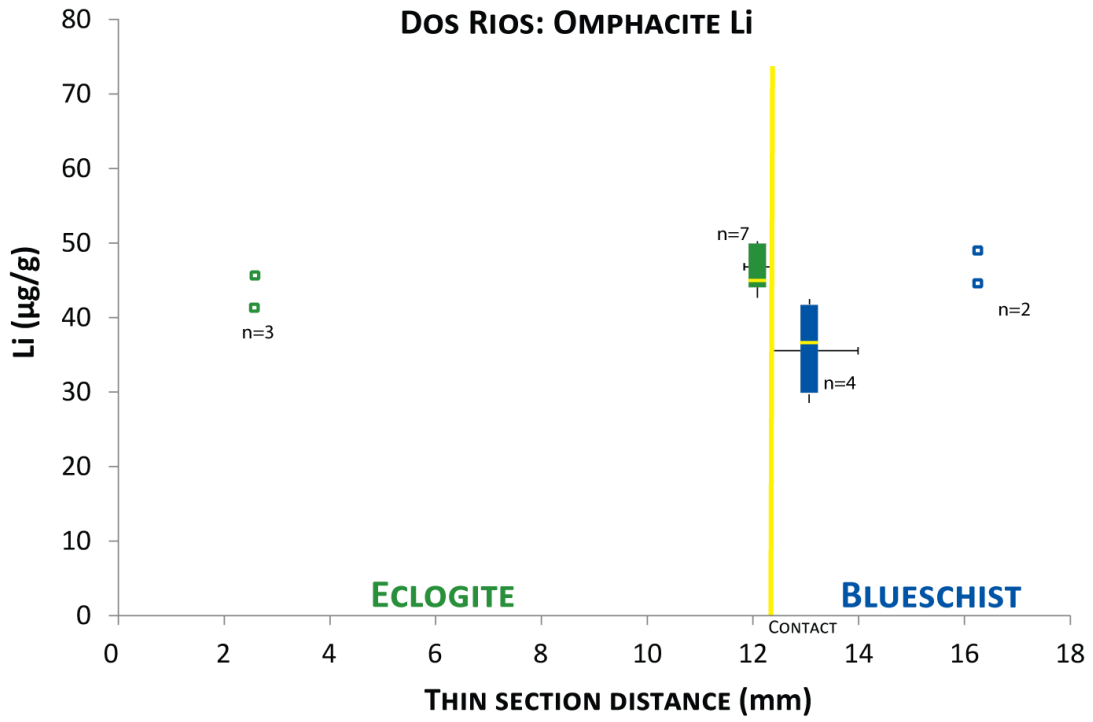


Figure 15. Dos Rios omphacite Li concentrations.

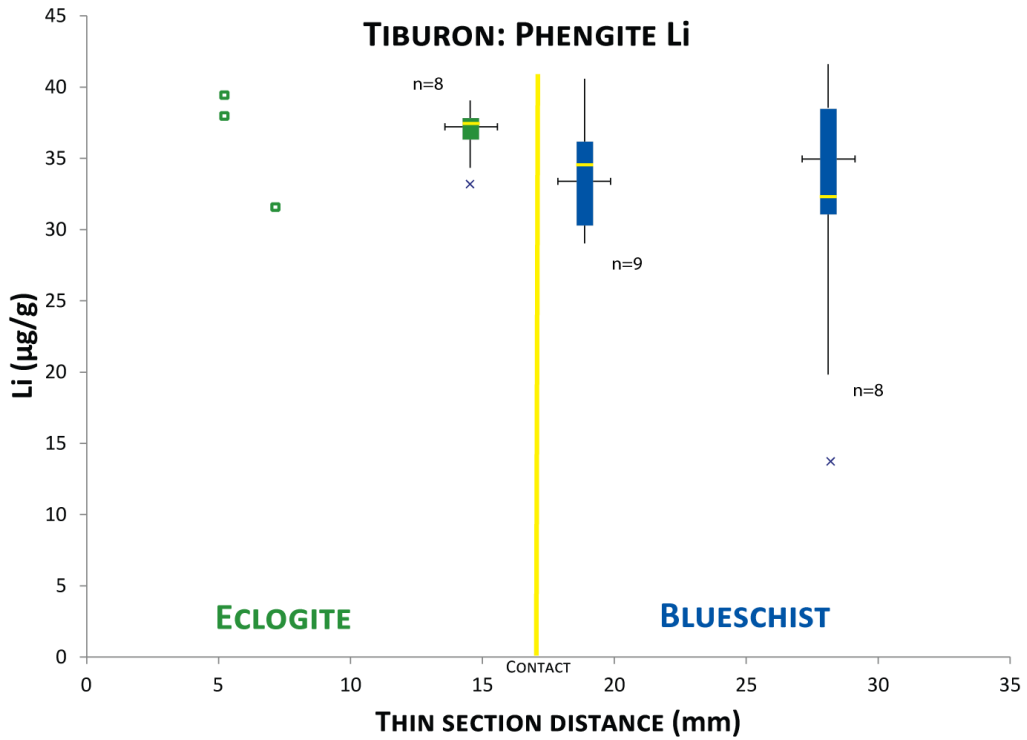


Figure 16. Tiburon phengite Li concentrations.

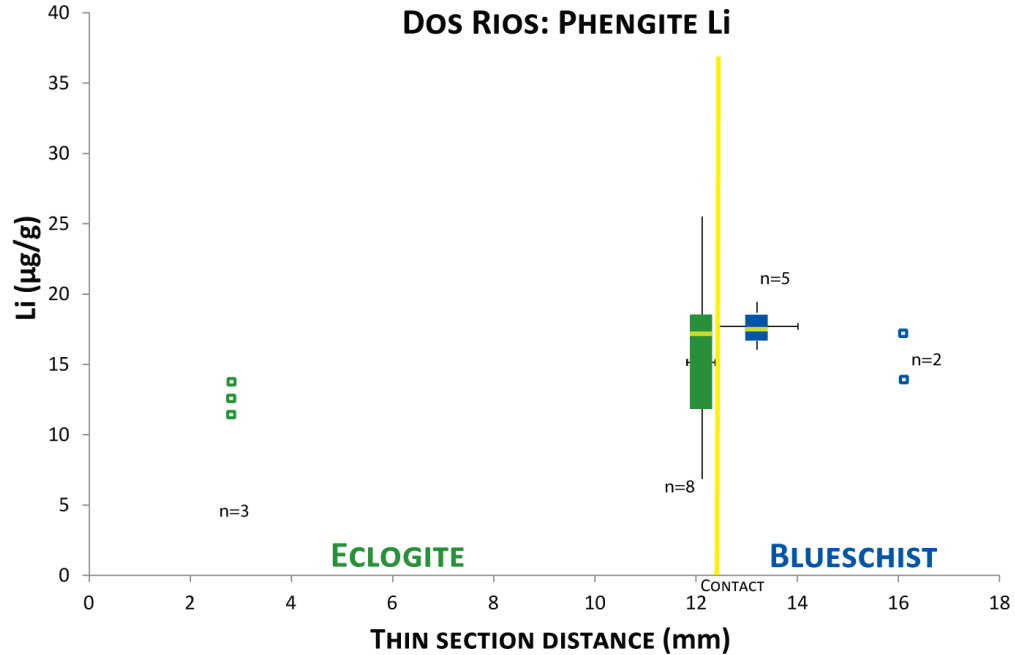


Figure 17. Dos Rios phengite Li concentrations.

Dos Rios phengites have an average Li concentration of phengites is $14 \pm 5.0 \mu\text{g/g}$ in the eclogite portion of the sample and $16 \pm 4.5 \mu\text{g/g}$ in the blueschist portion of the sample (Figure 17). The t-test yielded a p-value of 0.3, indicating that the difference between eclogite and blueschist are not statistically significant.

4.3.4 Chlorite

Tiburon chlorites have an average Li concentration of $82 \pm 6.2 \mu\text{g/g}$ in the eclogite portion of the sample and $69 \pm 9.2 \mu\text{g/g}$ in the blueschist portion of the sample (Figure 18). The t-test yielded a value of 0.003, indicating a statistically significant difference between eclogite and blueschist domains. There were not enough chlorites to measure in the Dos Rios sample to compare to the Tiburon sample.

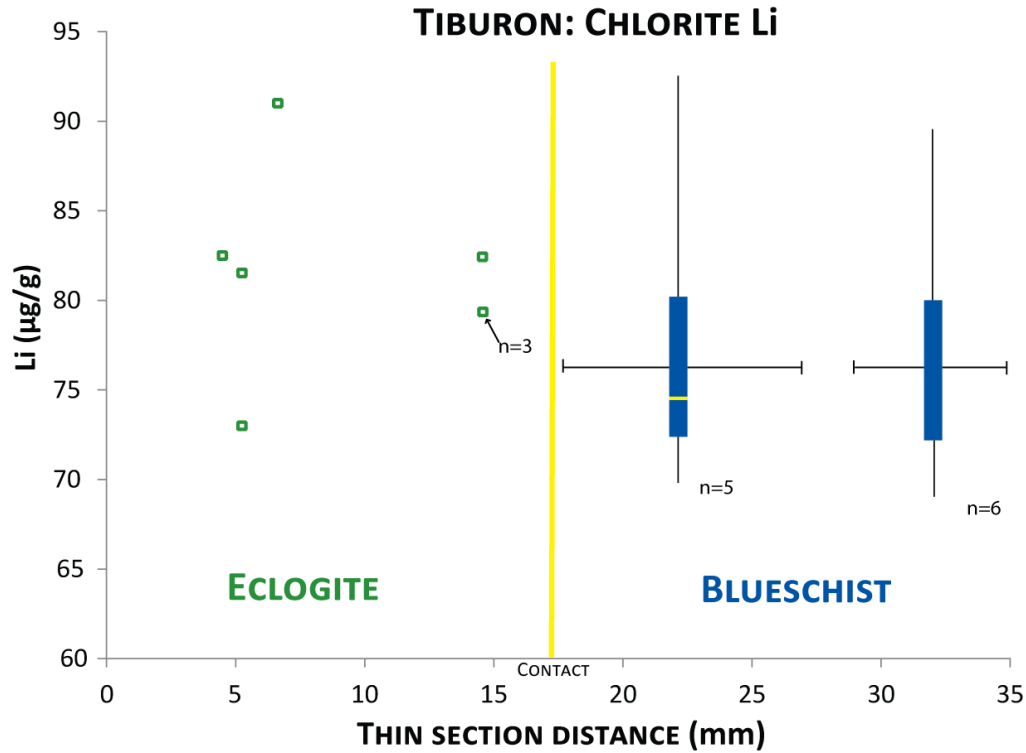


Figure 18. Tiburon chlorite Li concentrations.

4.3.5 Low-Li phases

The epidote in the Tiburon sample has an average Li concentration of 7.2 ± 1.2 $\mu\text{g/g}$ in the blueschist domain. No epidote was analyzed in the eclogite domain due to difficulties with differentiating between epidote and phengite phases in optical microscopy. The titanite has an average Li concentration of 4.1 ± 1.0 $\mu\text{g/g}$ in the eclogite domain and 4.8 ± 1.1 $\mu\text{g/g}$ in the blueschist domain. The garnet has an average Li concentration of 3.5 ± 1.1 $\mu\text{g/g}$ in the eclogite domain and 3.4 ± 1.1 $\mu\text{g/g}$ in the blueschist domain. In the Dos Rios sample, the epidote has an average Li concentration of 3.6 ± 0.5 $\mu\text{g/g}$ in the eclogite domain and 5.4 ± 1.6 $\mu\text{g/g}$ in the blueschist domain. The titanite has an average Li concentration of 3.4 ± 0.3 $\mu\text{g/g}$ in the eclogite domain and 5.4 ± 0.6 $\mu\text{g/g}$ in the blueschist domain. The garnet has an average

Li concentration of $2.9 \pm 0.01 \mu\text{g/g}$ in the eclogite domain and $2.7 \pm 0.2 \mu\text{g/g}$. Analyses only number 3-4 for each phase, there may not be enough data to differentiate between eclogite and blueschist domains in the two samples.

4.4 Bulk rock reconstruction

A reconstruction of the bulk rock Li concentration budget was calculated. Calculations were modeled after the bulk rock trace element reconstructions in Spandler et al. (2003). Briefly, the bulk rock reconstruction used the average Li concentration of each mineral and combined the Li concentration with the modal abundance of each mineral calculate its contribution to the bulk rock Li concentration. Bulk rock reconstruction of the Tiburon sample (Figure 19) shows that, in the eclogite domain, omphacite is the greatest contributor to the bulk Li concentration, followed by phengite, amphibole, chlorite, and the sum of the low-Li concentration phases. In the blueschist domain, the greatest contributor to the bulk Li concentration is amphibole, followed by phengite, chlorite, omphacite, and the sum of the low-Li concentration phases.

Bulk rock reconstruction (Figure 20) of the Dos Rios sample shows that, in the eclogite domain, omphacite is the greatest contributor to the bulk Li concentration, followed by amphibole, the sum of the low-Li concentration phases, and phengite. In the blueschist domain, the greatest contributor to the bulk Li concentration is amphibole, followed by phengite, omphacite, the sum of the low-Li concentration phases, and phengite. Omphacite is the greatest contributor to the bulk

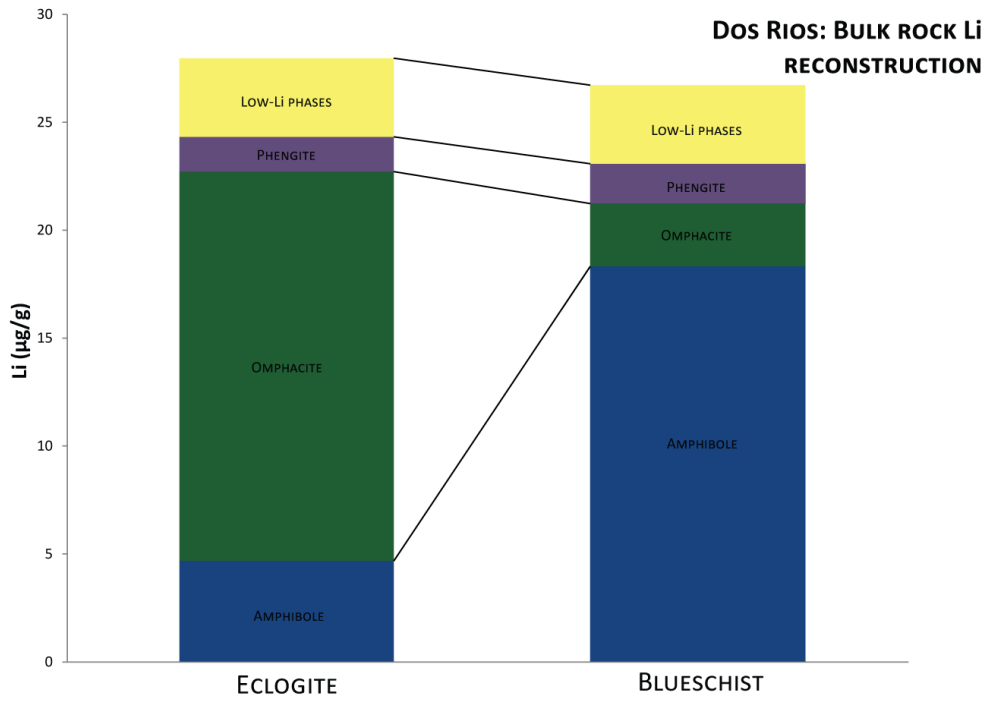


Figure 19. Tiburon bulk rock Li concentration reconstruction.

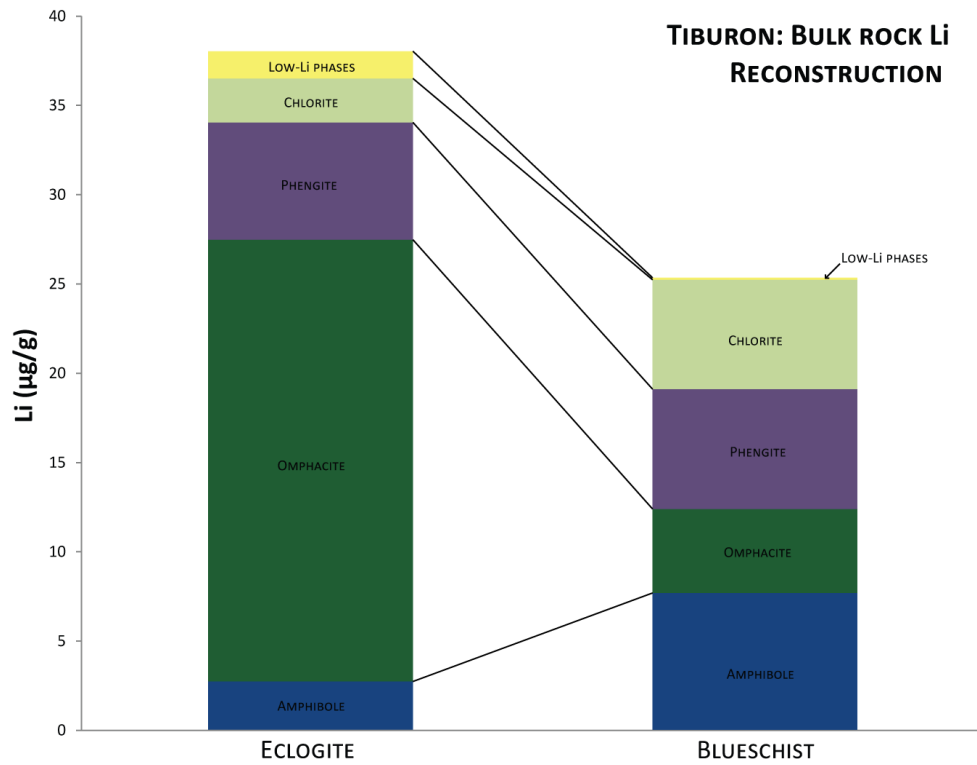


Figure 20. Dos Rios bulk rock Li concentration reconstruction.

Li concentration in the eclogite domain in both samples and amphibole is the greatest contributor to the bulk Li concentration in the blueschist domain of both samples.

Since omphacite has a higher average Li concentration than amphibole, it would follow that the bulk Li concentration of the eclogite would be higher than the bulk Li concentration of the blueschist, as shown in Figure 2.

5 Discussion

The Tiburon and Dos Rios samples differ texturally and geochemically. These variations are interpreted to be fluid-mediated alteration producing the cm-scale, eclogite and blueschist rock in the Tiburon sample and another mechanism producing the same alternating rock types in the Dos Rios sample. The following discussion will present evidence to support this interpretation and propose a possible mechanism to produce the alternating eclogite and blueschist layers in the Dos Rios sample.

5.1 Textural observations

Textural evidence suggesting fluid-mediated retrograde alteration is present in the Tiburon sample, but not in the Dos Rios sample. The Tiburon sample has garnets in the eclogitic domain that grade into chlorite-replaced garnet pseudomorphs in the blueschist domain over a distance of about 2 cm over the thin section, which is interpreted to be an indicator of fluid-rock interaction. The Dos Rios sample has no evidence of even partial chloritization of garnets, indicating that there was no fluid that altered the garnets in the blueschist domain. Moreover, chlorite is a major phase found in the blueschist domain in the Tiburon phase, comprising 10% of the volume of the blueschist. The blueschist domain in the Dos Rios sample contains no chlorite,

further showing that there was likely no fluid-rock interaction to produce chlorite.

Pumpellyite is another hydrous phase that exists in only in the blueschist domain of the Tiburon sample and not in the Dos Rios sample.

BSE imaging of the two samples shows further evidence for fluid-rock interaction. The omphacites in the Tiburon sample of the blueschist domain show high-Ca patches as well as some pumpellyite alteration. These textures are not seen in the omphacites of the Dos Rios sample blueschist domain, which is interpreted as evidence of a lack of fluid-alteration in the Dos Rios sample.

5.2 Major and minor element mineral compositions

The major and minor element compositions of the minerals in the Tiburon and Dos Rios samples are largely similar, with a few exceptions. The average composition of the omphacites varies between the two samples: the Tiburon samples are more jadeitic (i.e., more sodic) in composition (with an average 39% jadeite component), while the Dos Rios omphacites are more diopsidic (e.g., more calcic) in composition (with an average 31% jadeite component; note that the portions of the omphacite analyzed were not the altered diopside/pumpellyite patches). The phengites in the Tiburon sample are also more sodic in composition – the phengites in the Tiburon sample have 0.8 ± 0.2 wt.% Na_2O , and the phengites in the Dos Rios sample have 0.2 ± 0.1 wt.% Na_2O . the phengites of the two samples have a different Si content, ranging from 3.3-3.45 apfu in the Tiburon phengites, and 3.45-3.60 apfu in the Dos Rios phengites.

5.3 Li concentration analysis results

Measuring Li concentration in individual phases in each of the sample revealed some systematic differences between the Tiburon and Dos Rios samples. The two phases in the Tiburon sample that show textural differences indicating fluid-rock interaction – the omphacites and the chlorites – both systematically have higher Li concentration in the eclogite domain than in the blueschist domain (omphacite: $56 \pm 3.9 \mu\text{g/g}$ to $33 \pm 8.2 \mu\text{g/g}$; chlorite: $82 \pm 4.3 \mu\text{g/g}$ to $69 \pm 5.8 \mu\text{g/g}$). The Li concentration of the blueschist omphacites does not decrease near the contact, but rather decreases farther away from the contact. This differs from the Dos Rios sample in that the low Li concentration population is near located near blueschist/eclogite contact ($32 \pm 2.8 \mu\text{g/g}$, $n=6$). Omphacites farther away from the contact within the blueschist have a Li concentration that is indistinguishable from those in the eclogite ($45 \pm 2.4 \mu\text{g/g}$, $n=3$ compared to $46 \pm 2.8 \mu\text{g/g}$ in the eclogite). It is not clear why some omphacites in the blueschist domain in the Dos Rios sample are similar to the omphacites in the eclogite domain and others are different.

5.4 Comparison to other studies

Marschall et al. (2006) measured Li concentrations in a variety of high pressure subduction zone rocks from the island of Syros, Greece. Lithium concentrations were determined in the same phases as outlined in this study (glaucofane, clinopyroxene, chlorite, phengite, garnet, titanite, and epidote) via secondary ion mass spectrometry (SIMS). The ranges of Li concentration measured in

the phases in this study are comparable with the ranges found in this study. Table 3 compares the Li concentration results in this study and in Marschall et al. (2006).

Li concentration in phase (ug/g)	Clinopyroxene/ Omphacite	Phengite	Glaucophane	Chlorite
This study	33-56	14-37	16-31	69-82
Marschall et al., 2006	6.81-130	2.57-48.7	5.94-115	3.45-115

Table 6. Range of Li concentrations measured in this study for individual minerals in this study and in Marschall et al. (2006).

All of the Li concentrations measured in this study overlap with the range of Li concentrations measured in the Marschall et al. (2006) study. The minerals analyzed in the Marschall et al. (2006) study are much more variable in their range of Li concentrations than in this study. Both studies show that clinopyroxene (omphacite), gualcophane, phengite, and chlorite have the bulk of the Li concentration – 94% of the Li concentration budget in this study and 95% of the budget in the Marschall et al. (2006) study (refer to previous section on bulk rock Li concentration reconstruction).

5.5 Possible mechanisms for coexisting blueschist and eclogite in Dos Rios sample

This study has outlined a variety of textural, mineralogical, and geochemical differences between the Tiburon sample, which has evidence for fluid-mediated alteration, and the Dos Rios sample, which does not. One way to produce differences in mineralogy and geochemistry without fluid-rock interactions would be to have a different protoliths for the eclogite and blueschist. For instance, blueschist facies metagreywackes in the Catalina Schist (a related subduction zone complex in California) can have mineral assemblages that have some overlap with the Dos Rios

blueschist assemblages (e.g., Platt, 1975). However, the high field strength element (HFSE) composition of the rocks show that most Franciscan blocks – including the ones in this study – are similar in composition to mid-ocean ridge basalts, indicating that this is the blocks’ most likely protolith (Sorensen et al., 1997). In addition, the high-grade blocks of the Franciscan Complex have a ϵ_{Nd} of 9.3 ± 1.4 , indicating that the protoliths had a normal depleted-mantle source (Nelson, 1995). Moreover, various studies that have looked at blueschist recrystallized from metagraywacke have found that there are different mineral phases that recrystallize that are not found in metabasalts; i.e., lawsonite instead of epidote as the CaAl favored CaAl silicate; significant amounts of quartz and albite, greater amounts of calcite and aragonite; and little glaucophane (e.g., Ernst, 1963; Ghent, 1965; Blake, 1967; Platt, 1975). Therefore, the chemistry and mineralogy of the Dos Rios blueschist domain is not consistent with a different protolith from the eclogite domain.

The most likely reason for the alternating blueschist and eclogite domains in the Dos Rios sample is variations in bulk composition in the original mafic rocks. Coleman and Lanphere (1971) recognized high-grade blocks with eclogite layers “contemporaneous and in apparent equilibrium” interlayered with blueschist with no apparent retrograde features, similar to the Dos Rios sample of this study. Coleman and Lanphere (1971) commented on the interlayered blueschist and eclogite layers:

“There seems little reason to doubt that garnet-omphacite (eclogite) layers of larger masses crystallized at the same time as the associated blueschists. The variation in mineral assemblages is a function of bulk composition and, perhaps, of the availability of water (p. 2404).”

Moore and Blake (1989) also recognized that the the metamorphic textures of high grade blocks of the Franciscan Complex showed that the eclogite and blueschist can form at the same time. These blocks metamorphosed from a mafic protolith to a hornblende schist and then to blueschist and eclogite. The blueschist and eclogite domains replaced the original hornblende with glaucophane simultaneously, showing that the blueschist and eclogite simultaneously recrystallized. They also hypothesized that the simultaneous formation of blueschist and eclogite was due to differences in bulk chemistry of the protolith.

Brovarone et al. (2011) also proposed that coexisting eclogite and blueschist rock can arise as a result of variations in bulk rock composition of the mafic protolith. This study reported bulk rock compositions of coexisting eclogite and blueschist rock from Alpine Corsica, France using ICP-MS. Based on the bulk rock compositions, phase equilibria diagrams were calculated to determine the P-T conditions in which the two lithologies were stable. The study found that a higher CaO content strongly affects the formation of omphacite versus glaucophane under high P-T conditions – a higher CaO content favors the formation of eclogite rather than blueschist under the same P-T conditions. Brovarone et al. (2011) favor the suggestion in Seyfried et al. (1988) that demonstrated that CaO depletion in the original mafic protolith can arise from shallow seafloor alteration. The CaO composition of the eclogite and blueschist of the Dos Rios sample in this study are consistent with the mechanism proposed by Brovarone et al. (2011) – the eclogite portion of the rock has a higher average bulk CaO composition (12.1 ± 0.8 wt.% [Sorensen et al., 1997; average and σ_m of all eclogite layers of DR block]; c.f. 14.35

wt% in Brovarone et al., 2011) than the blueschist portion of the rock (10.9 ± 0.1 wt.% [Sorensen et al., 1997; average and $1\sigma_m$ of all blueschist layers of DR block]; cf. 10.95 wt% in Brovarone et al., 2011).

Altered basalts can be found throughout the Franciscan complex, and have a wide range of igneous textures, including tuffs, pillows, and breccias. Pillows are widespread throughout the complex, and range from sub-meter sized to several hundred meters in size (Bailey et al., 1964). These pillows commonly have features consistent with shallow sea-floor alteration, including zeolitization and spilitization. Bailey et al. (1964) analyzed unaltered Franciscan pillow cores and rinds that appear to have undergone seafloor alteration. They determined that CaO and Na₂O decreased going from unaltered core to altered rind (15.8 to 8.5 wt. % and 3.1 to 2.7 wt. %, respectively), while FeO and MgO increased going from core to rind (4.4 to 6.6 wt. % and 4.8 to 7.9 wt.%, respectively). They attribute this change in bulk rock chemistry to differences in temperatures between rind and core when the pillow basalt erupted. After eruption, the rind cooled quickly, and sealed off the core from sea water interaction. The large difference in temperature allowed for sufficient time for major element migration to occur. Other studies also found CaO depletion going from unaltered core to altered rind in pillow basalts (Vuagnat, 1946, 1949). These bulk rock core-rind analyses are compatible with the experiments done in Seyfried et al. (1988).

Based on these previous studies, I propose that eclogite and blueschist domains in the Dos Rios sample may have formed as a result of variations in the original mafic protolith. As Bailey (1964) and Vuagnat (1946, 1949) found, pillow

basalts may undergo alteration when exposed to seawater, which can differentiate CaO between unaltered core and altered rind. When metamorphosed at the same pressure and temperature conditions, the CaO enriched core will recrystallize to eclogite and the CaO depleted rind will recrystallize to blueschist, as found in the Brovarone et al. (2011) study. The multiple, interlayered blueschist and eclogite rock in the Dos Rios may have formed as a result of alteration along fractures in the original pillow basalt. Pillow basalts may fracture when erupted on the seafloor. Seawater can move along these fractures and alter the basalts along the fractures, while leaving the cores intact (Miller et al., 2000, 2001). Brovarone et al. (2011) notes that the metamorphosed pillows analyzed have an eclogite mineral assemblage in the core and a blueschist assemblage in the cores. Another mechanism that could produce the interlayered eclogite and blueschist could be several smaller pillow basalts pushed together and metamorphosed together.

The Dos Rios sample does not have as dramatic of a difference between CaO in eclogite and blueschist domains (12.1 ± 0.8 wt.% and 10.9 ± 0.1 wt.%; Sorensen et al, 1997) as in the Brovarone, et al., (2011) study, nor in the basalts in Bailey et al., (1964) or Vuagnat (1946, 1949) studies. However, in the absence of evidence of other mechanisms that could produce cm-scale eclogite and blueschist (e.g., P-T differences and/or fluid-mediated alteration), differences in bulk mafic composition are probably the most likely mechanism. The Tiburon sample has a larger difference in CaO in eclogite vs blueschist (11.9 vs 7.0 wt.%). Although there still may have been a difference in the mafic protolith in the Tiburon sample, textural evidence suggests that fluid-mediated alteration may have produced the differences in chemical

composition. There is not a sharp contact between eclogite and blueschist compositions, as in the Dos Rios sample; instead, fluid-mediated eclogite phases seem to gradationally alter into the blueschist domain. For example, as in Figure 4, the garnets appear to become more chloritized farther away from the contact, indicating that the entire rock was eclogite and the fluid-mediated reactions did not to go completion closer to the contact.

6 Conclusions

The Tiburon and Dos Rios samples both have coexisting cm-scale blueschist and eclogite domains. Textural and geochemical evidence demonstrates that differing mechanisms produced the coexisting lithologies. Textural evidence includes:

- a) Chlorite after garnet pseudomorphs in the blueschist domain of the Tiburon sample that indicate fluid-mediated alteration of the eclogite.
- b) Pumpellyite in the blueschist domain of the Tiburon sample, another hydrous phase that indicates retrograde fluid-mediated alteration.
- c) Omphacites in the eclogite domain of the Tiburon sample appear relatively homogenous in BSE, while omphacites are altered to diopside and pumpellyite patches in the blueschist domain.

Both samples have different Li concentration. The concentration of Li in both chlorite and omphacite in the Tiburon sample decreases going from eclogite to blueschist domains. These phases appear to have recrystallized going from eclogite to blueschist, so it is likely that the lower Li concentration of these phases is a result of fluid-mediated alteration. The Li concentration of the phases of the Dos Rios sample

does not change significantly going from eclogite to blueschist domains, so the mechanism that produced the alternating lithologies is different from the Tiburon sample. I infer that the trends in Li concentration and the petrological observations are the result of the infiltrating fluid imparting a different Li concentration to the minerals in the blueschist layer compared to the original eclogite. The alternating blueschist and eclogite domains in the Dos Rios sample likely arise from a heterogeneous bulk rock composition of the protolith basalt that underwent seafloor alteration.

The techniques used and the results of this study can be applied in a number of different ways. The results of this study suggest that Li concentration analyses can be used as a monitor of fluid-rock interactions in subduction zone metamorphic rocks. The ability to track fluid behavior in rocks can be also useful in a variety of geological settings besides subduction zones – i.e., fluid-rock interactions in other parts of the upper and lower crust. Other techniques that could be used in this study include Li isotopic analyses of mineral separates in both samples to compare the Li isotopic signatures of the two samples. The bulk rock $\delta^7\text{Li}$ of the blueschist layer is higher than the associated eclogite layer for both the Tiburon and Dos Rios samples (Penniston-Dorland et al., 2010). The results from Penniston-Dorland et al. (2010) suggest that the difference in bulk rock $\delta^7\text{Li}$ between blueschist and eclogite in the Tiburon sample is due to fluid-mediated alteration. Based on the results of this study and of Penniston-Dorland et al. (2010), I predict that individual mineral phases in the Tiburon sample for which the Li concentration is altered by fluid-rock interaction would also have a higher $\delta^7\text{Li}$ in the blueschist layer than the eclogite layer. The

results of this study suggest that the bulk rock difference in $\delta^7\text{Li}$ for the Dos Rios sample is the effect of different abundances of different mineral phases, so the predicted result of analysis of mineral separates is that they will have similar $\delta^7\text{Li}$ in blueschist and eclogite.

7 Appendices

7.1 Appendix A: Tiburon data tables

Refer to supplemental spreadsheet: tiburon supplemental.xlsx

7.2 Appendix B: Dos Rios data

Refer to supplemental spreadsheet: dos rios supplemental.xlsx

7.3 Appendix C: Accuracy and precision data

Refer to supplemental spreadsheet: accuracy and precision supplemental.xlsx

8 References

- Bailey, E.H, Irwin, W.P., and Jones, D.L., 1964. Franciscan and related rocks, and their significance in the geology of western California. *Ca. Div. Mines and Geol. Bull.*, 183, pp. 1-177.
- Bebout, G.E., 2007. Metamorphic chemical geodynamics of subduction zones. *Earth Planet. Sci. Lett.*, 260, pp.373-93.
- Blake, M.C., Irwin, W.P. & Ghent, E., 1967. Regional glaucophane schist-facies metamorphism in the northern Coast Ranges of California (abs). *Geol. Soc. Spec. Paper*, 82, pp.241.
- Brenan, J.M., Ryerson, F.J. and Shaw, H.F., 1998. The role of aqueous fluids in the slab-to-mantle transfer of boron, beryllium, and lithium during subduction: experiments and models. *Geochim. Cosmochim. Acta*, 62(19/20), pp.3337-47.
- Brovarone, A.V., Gropo, C., Hetenyi, G., Compagnoni, R. and Malavieille, J., 2011. Coexistence of lawsonite-bearing eclogite and blueschist: phase equilibrium modelling of Alpine Corsica metabasalts and petrological evolution of subducting slabs. *J. Meta. Geol.*, 29, pp.583-600.
- Catlos, E.J. and Sorensen, S.S., 2003. Phengite-based chronology of K- and Ba-rich fluid flow in two paleosubduction zones. *Science*, 299, pp.92-95.
- Cloos, M., 1983. Comparative study of melange matrix and metashales from the Franciscan Subduction Complex with the basal Great Valley Sequence, California. *J. Geol.*, 91(3), pp.291-306.
- Cloos, M., 1986. Blueschists in the Franciscan Complex of California: petrotectonic constraints on uplift mechanisms. *Mem. Geol. Soc. Amer.*, 164, pp.77-93.
- Coleman, R.G. and Lanphere, M.A., 1971. Distribution and age of high-grade blueschists, associated eclogites, and amphibolites from Oregon and California. *Geol. Soc. Am. Bull.*, 82, pp.2397-412.
- Ernst, W.G., 1963. Petrogenesis of glaucophane schists. *Jour. Petrology*, 4, pp.1-30.
- Giaramita, M.J. and Sorensen, S.S., 1994. Primary fluids in low-temperature eclogites: evidence from two subduction complexes (Dominican Republic, and California, USA). *Contrib. Mineral Petrol.*, 117, pp.279-92.
- Ghent, E., 1965. Glaucophane schist facies in the Black Butte area, Northern Coast Ranges, California. *Am. Jour. Sci.*, 263, pp.385-400.
- Hawthorne, F.C. and Oberti, R., 2007. Classification of the amphiboles. *Rev. Min. Geo.*, 67, pp.55-88.
- Liou, J.G., Maruyama, S. and Moonup, C., 1987. Very low-grade metamorphism of volcanic and volcanoclastic rocks - mineral assemblages and mineral facies. In M. Frey, ed. *Low grade metamorphism*. 1st ed. London: Blackie and Son, Limited. pp.59-112.
- Manning, C.E., 2004. The chemistry of subduction zone fluids. *Earth Planet. Sci. Lett.*, 223, pp.1-16.
- Marschall, H.R., Altherr, R., Ludwig, T., Kalt, A., Gmeling, K. and Kaszovszky, Z., 2006. Partitioning and budget of Li, Be, and B in high-pressure metamorphic rocks. *Geochim. Cosmochim. Acta*, 70, pp.4750-69.

- Marschall, H.R., Pogge von Strandmann, P.A., Seitz, H.-M., Elliot, T. and Niu, Y., 2007. The lithium isotopic composition of orogenic eclogites and deep subducted slabs. *Earth Planet. Sci. Lett.*, 262, pp.563-80.
- Moore, D.E. and Blake, M.C., 1989. New evidence for polyphase metamorphism of glaucophane schist and eclogite exotic blocks in the Franciscan Complex, California and Oregon. *J. Meta. Geol.*, 7(2), pp.211-28.
- Nelson, B.K., 1991. Sediment-derived fluids in subduction zones: Isotopic evidence from veins in blueschist and eclogite of the Franciscan Complex, California. *Geology*, 19, pp.1033-36.
- Nelson, B.K., 1995. Fluid-flow in subduction zones-evidence from Nd and Sr-isotope variations in metabasalts of the Franciscan Complex, California. *Contrib. Mineral. Petrol.*, 119, pp.247-62.
- Penniston-Dorland, S.C., Sorensen, S.S., Ash, R.D. and Khadke, S.V., 2010. Lithium isotopes as a tracer of fluids in a subduction zone melange: Franciscan Complex, CA. *Earth Planet. Sci. Lett.*, 260, pp.181-90.
- Platt, J.P., 1975. Metamorphic and deformational processes in the Franciscan Complex, California: Some insights from the Catalina Schist terrane. *Geol. Soc. Bull.*, 86(10), pp.1337-47.
- Ruxton, G.D., 2006. The unequal variance t-test is an underused alternative to Student's t-test and the Mann-Whitney U test. *Behavioral Ecology*, 17(4), pp. 688-690.
- Seyfried, W.E., Ding, K. and Berndt, M.E., 1988. Phase equilibria constraints on the chemistry of hot spring fluids at mid-ocean ridges. *Geochim. Cosmochim. Acta*, 55, pp.3559-80.
- Sorensen, S.S., Grossman, J.M. and Perfit, M.R., 1997. Phengite-hosted LILE enrichment in eclogite and related rocks: implications for fluid-mediated mass transfer in subduction zones and arc magma genesis. *J. Petrol.*, 38(1), pp.3-34.
- Spandler, C., Hermann, J., Arculus, R. and Mavrogenes, J., 2003. Redistribution of trace elements during prograde metamorphism from lawsonite blueschist to eclogite facies; implications for deep subduction-zone processes. *Contrib. Mineral. Petrol.*, 146, pp.205-22.
- Teng, F.Z., McDonough, W.F., Rudnick, R.L. and Walker, R.J., 2006. Diffusion-driven extreme lithium isotopic fractionation in country rocks of the Tin Mountain pegmatite. *Earth Planet. Sci. Lett.*, 243, pp.701-10.
- Teng, F.-Z., Rudnick, R.L., McDonough, W.F., Gao, S., Tomascak, P.B. and Liu, Y., 2008. Lithium isotopic composition and concentration of the deep continental crust. *Chem. Geol.*, 255, pp.47-59.
- Van Der Plas, L. and Tobi, A.C., 1965. A chart for judging the reliability of point counting results. *Am. J. Sci.*, 263, pp.87-90.
- Vuagnat, M., 1946. Sur quelques diabases suisses. Contribution a l'etude du probleme des spilites et des pillow lavas. *Schweizer Miner. Petrogr. Mitt.*, 26(2), pp. 116-228.
- Vuagnat, M., 1949. Variolites et spilites. Comparison entre quelques pillow lavas britanniques et alpines. *Archives des Science*, 2(2), pp. 223-236.

- Wakabayashi, J., 1990. Counterclockwise P-T-t paths from amphibolites, Franciscan Complex, California: Relics from the early states of subduction zone metamorphism. *J. Geol.*, 98(5), pp.657-80.
- Wunder, B., Meixner, A., Romer, R.L., Feenstra, A., Schettler, G. and Heinrich, W., 2007. Lithium isotope fractionation between Li-bearing staurolite, Li-mica and aqueous fluids: An experimental study. *Chem. Geol.*, 238, pp.277-90.
- Wunder, B., Meixner, A., Romer, R.L. and Heinrich, W., 2006. Temperature-dependent isotopic fractionation of lithium between clinopyroxene and high-pressure hydrous fluids. *Contrib. Mineral. Petrol.*, 151, pp.112-20.
- Zack, T., Tomascak, P.B., Rudnick, R.L., Dalpe, C. and McDonough, W.F., 2003. Extremely light Li in orogenic eclogites: the role of isotope fractionation during dehydration in subducted oceanic crust. *Earth Planet. Sci. Lett.*, 208, pp.279-90.